Energetic Nitrogen Ions within the Inner Magnetosphere of Saturn

By

E.C. Sittler Jr.[1], R.E. Johnson,[2] H.T. Smith[2], J.D. Richardson[3], S. Jurac[3], M. Moore[1], J.F. Cooper[4], B. H. Mauk[5], M. Michael[2], C. Paranicas[5], T. P. Armstrong[6], and B. Tsurutani[7]

1. **NASA/Goddard Space Flight Center/Greenbelt, MD**
2. **University of Virginia/Charlottesville, VA**
3. **Massachusetts Institute of Technology/Cambridge, MA**
4. **Raytheon Technical Services Company LLC, NASA Goddard Space Flight Center, Greenbelt, MD**
5. **Applied Physics Laboratory/Laurel, MD**
6. **Fundamental Technology, Lawrence, KS**
7. **Jet Propulsion Laboratory, Pasadena, CA**

ABSTRACT

Titan's interaction with Saturn's magnetosphere and dissociation of N_2 in Titan's atmosphere by electrons and UV photons cause ejection of nitrogen atoms into Saturn's outer magnetosphere. This results in the formation of a torus of neutral nitrogen at Titan's orbit with a source strength of about 4.5×10^{25} atoms/sec and a mean density of about 4 N/cm^3. The theoretical estimate of the source strength of the ejected nitrogen atoms has varied by more than an order of magnitude over a span of more than 20 years. This can be traced to an uncertainty in the position of the ionopause relative to the exobase at Titan. If the ionopause is above the exobase the source term will be lower, while if it is near or below the exobase it will be higher. A lower height to the ionopause will allow the magnetospheric plasma to have access to Titan's upper atmosphere and thus produce more energetic nitrogen atoms. The nitrogen in the torus is ionized by photons, electrons and charge exchange producing an N^+ torus of 1-4 keV suprathermal ions centered on Titan's orbital position. We show that the Voyager plasma instrument detected the presence of a heavy suprathermal ion component within Saturn's outer magnetosphere. The plasma instrument also detected a time dependent denser cold ion component within the outer magnetosphere, which could either be O^+ or N^+ or both. The cold O^+ would come from the inner magnetosphere, while the cold N^+ could come from the scavenging of Titan's ionospheric plasma by Saturn's magnetospheric flow. A cold proton component was also detected. The Voyager Low Energy Charged Particle (LECP) experiment data also indicated the presence of inward diffusing energetic ions for which we argue to have an N^+ contribution from the outer magnetosphere of Saturn, but a proton component cannot be excluded and may very well dominate at high latitudes above the plasma sheet. Conserving the first and second adiabatic invariants such ions would have energies in excess of 100 keV at Dione's L shell and greater than 400 keV at

Enceladus' L shell. Energetic charged particle radial diffusion coefficients are used as constraints. Initial estimates indicate that a solar wind source of protons and alpha particles could dominate in the outer magnetosphere, but the parameters needed are highly uncertain and will have to await Cassini results for confirmation. Using radial diffusion coefficients that do not violate observations and Voyager magnetometer measurements at Rhea's L shell, we find that satellite sweeping and charged particle precipitation within the middle and outer magnetosphere enrich inwardly diffusing N^+ ions relative to protons in Saturn's inner magnetosphere. Ion cyclotron waves can isotropize the protons, but both PLS and LECP data argue for pancake distributions for the heavy ion suprathermal component so that radial diffusion must be relatively fast. This is also supported by modeling of the HST observations of the OH cloud in Saturn's inner magnetosphere. E-ring absorption is negligible, but charged exchange reactions can be an important loss mechanism in the inner magnetosphere for energetic protons and heavy ions. Composition data at energies greater than 200 keV/nucl., earlier on suggested that O^+ ions within Saturn's inner magnetosphere dominated over protons, and that sputtering of icy moons and rings provided a potential source of O^+. However, we now argue that N^+ ions from Titan may dominate the energetic ion population within the inner magnetosphere such that protons dominate at high latitudes and that heavy ions, such as N^+, dominate in the equatorial plane (i.e., $T_\perp/T_{ll} >> 1$ for N^+, while protons are isotropic). A source of hot keV O^+ ions within Saturn's outer magnetosphere could also be competitive with Titan's nitrogen torus (Eviatar et al. (1983)). The observations are consistent with the interpretation that the pickup heavy ions, confined to regions where neutral clouds exist, produce ion cyclotron waves which will be in resonance with energetic protons, but not energetic heavy ions. Therefore, energetic protons are preferentially isotropized and precipitated relative to energetic heavy ions within those regions where neutral clouds exist. We also show that charge exchange losses will enrich N^+ ions relative to protons within Saturn's magnetosphere. Bombardment of the icy satellite surfaces by N^+ can cause chemical reactions in the ice and nitrogen products can accumulate in the ice over the lifetime of the Saturn system. We present a new analysis of the Voyager PLS and LECP data sets at both Titan's nitrogen torus and Dione's L shell and make predictions for the Cassini Mission on the possible detection of suprathermal N^+ ions, implantation of energetic nitrogen ions in the surfaces of the icy satellites, nitrogen molecules sputtered from satellite surfaces and picked up in the corotating plasma after ionization, and the radiolytic chemistry driven within the icy surfaces by the impacting energetic nitrogen ions.

1.0 **INTRODUCTION**

Data from Pioneer and Voyager flybys of Saturn showed that the magnetosphere contained a significant population of trapped, energetic (>10keV) heavy ions. The heavy ions are of interest as these likely come from sources orbiting in Saturn's magnetosphere and act as agents for chemical change and erosion via surface sputtering, implantation, and radiolysis of objects embedded in Saturn's magnetosphere. However, the principal source of these energetic heavy ions is controversial. Saturn's atmosphere and the solar wind are sources of light ions, while the icy moons and rings are sources of water molecules. On dissociation and ionization this results in a corotating O^+ plasma in the inner magnetosphere. As in the Jovian system such ions can go through a charge exchange cycle, propagate freely outward as neutrals, become ionized again by photo-ionization and becomes a source of energetic heavy ions via inward diffusion and acceleration. This mechanism could make energetic O^+ ions within Saturn's inner magnetosphere. Eviatar et al. (1983), suggested that charge exchange reactions between co-rotating O^+ ions and atomic hydrogen at the outer edge of the A-ring ($r \sim 2.25\ R_S$), might produce a source of neutral oxygen within Saturn's outer magnetosphere ($11.2 < r < 29.1\ R_S$) with a source strength as large as $S_O \sim 1.4x10^{26}$ atoms/s. If correct this could exceed by a factor of 2 our estimate of the nitrogen torus being discussed here. Johnson et al. (1989) also suggested recycling of water products by low energy orbiting collisions inside of the orbit of Enceladus. Cassini plasma composition data can resolve this. On charge exchange, oxygen in the so-called OH neutral torus will escape from the Saturn system. In competition with this process and advocated in this paper, is that Titan will provide a significant source of nitrogen into Saturn's outer magnetosphere forming a giant torus of neutral nitrogen. The source strength is estimated to be $S_N \sim 4.5x10^{25}$ atoms/s. When ionized this toroidal gas becomes a source of plasma ions. A fraction of these ions diffuse inward and become a source of energetic heavy ions for the inner magnetosphere.

Because the Voyager LECP instrument could not discriminate between O^+ and N^+, the relative contributions from these principal sources of heavy ions could not be identified. Early models suggested Titan was the dominant source (Barbosa, 1987). Later it was assumed that the heavy ions dominate the energetic plasma and, hence, that water products from sputtering of the icy satellites and E-ring grains would be a dominant source (Johnson et al., 1989). Recent examinations of Voyager LECP data have suggested far fewer energetic heavy ions and, hence, lower sputtering rates than were assumed earlier (Jurac et al. 2001; Paranicas et al, 2004). While, it is clear that the thermal plasma is dominated by water products, we will show that in the inner magnetosphere the energetic ion data are more consistent with protons dominating at higher latitude and N^+ may dominant near the ring plane We show this by re-examining Voyager data and using recent results on the sputtering of Titan's atmosphere. If true, then heavy ions may still dominate the sputtering rates for the icy satellites as originally thought, since the satellites are in the ring plane where energetic N^+ is expected to be more important.

With regard to the thermal plasma, water group ions will tend to dominate inside of Rhea's L shell, while outside of Rhea's L shell N^+ may dominate. But, the recent modeling of Titan's nitrogen torus by Smith et al. (2004), indicates a significant source of pickup N^+ ions could extend in as close as Dione's L shell. Finally, radial diffusion will tend to mix these two populations making the boundary diffuse in radial distance.

We first review the analysis of the Titan source rate and then describe the results of the most recent model for loss of atmosphere from Titan and the resultant formation of a neutral and plasma torus. We then re-examine the Voyager data and re-analyze the various sources of plasma for Saturn's magnetosphere. An examination of the loss processes follows. Although the nitrogen source strength is small, the loss processes are selective so that nitrogen is enriched relative to protons during inward diffusion. Finally we examine the situation at Dione as indicated by Voyager and we consider the effect of the energetic nitrogen on the surface of Dione. These results are used to make predictions which can be tested by data from Cassini.

1.1 Titan's Neutral Torus: Review of Models

Strobel and Shemansky (1982) studying Voyager 1 UVS data at Titan (see Broadfoot et al., 1981) identified EUV emissions consistent with electron impact dissociation of N_2 at Titan's exobase and the corresponding ejection of energetic nitrogen atoms from Titan. They suggested that these nitrogen atoms would form a giant nitrogen torus around Saturn with a source strength $S_N \sim 3 \times 10^{26}$ atoms/sec. This was followed by papers based on Voyager plasma observations by Eviatar et al. (1983) and Eviatar and Podolak (1983), for which, the latter paper estimated an atomic nitrogen source strength of $S_N \sim 7.5 \times 10^{25}$ atoms/sec. Further support of these studies was offered by Hunten et al. (1984) who showed that Titan should be an important source of neutral atoms and molecules within Saturn's magnetosphere, while Hunten (1982) and Johnson (1994) showed that nonthermal mechanisms were important for atmospheric escape from Titan. Barbosa (1987) estimated the dimensions of this atomic nitrogen torus based on ejection speeds at the exobase of 1-2 km/sec and on a source strength of $S_N \sim 6 \times 10^{26}$ atoms/sec. He also estimated that the torus would have radial extent between 8 R_S and 25 R_S and thickness between 8 R_S and 16 R_S depending on the assumed ejection velocities and an average nitrogen density of 6 atoms/cm^3. They then argued that the atomic nitrogen atoms would be ionized with a time scale $\tau \sim 3 \times 10^7$ sec and that the nitrogen N^+ ions would have pickup energies of several keV forming a suprathermal component for the ambient ions as observed by the Voyager plasma instrument (Lazarus and McNutt, 1983). It was argued that these suprathermal pickup nitrogen ions would then accelerate thermal electrons to energies ~ 1 keV via wave-particle interactions by lower hybrid waves (Barbosa, 1986). This prediction was supported by Voyager plasma electron observations (Sittler et al. (1983)). Barbosa (1987) further argued that the magnetometer results reported by Connerney et al. (1983) with Z3 internal field and ring current supported the mapping of field lines within the Titan torus to around 80° latitude at Saturn where the aurora was observed (Broadfoot et al., 1981; Sandel et al., 1982). The pickup energy of the suprathermal nitrogen ions within the Titan torus could provide a power level ~ 2 x 10^{11} watts for the precipitating keV electrons that would power the aurora as required by

the Voyager UVS observations (Sandel and Broadfoot, 1981). Sandel and Broadfoot (1981) also found the auroral emissions were consistent with Saturn's kilometric radiation (Warwick et al., 1981) for which the UV aurora was brightest at a sub-solar longitude ~ 100°. The importance of an internal energy source for producing the aurora and SKR is also supported by the theoretical considerations by Curtis et al. (1986), who considered the centrifugally driven flute instability.

The source strength of the ejected nitrogen atoms was revised downward by Strobel et al. (1992) from the original analysis by Strobel and Shemansky (1982) to $S_N < 10^{25}$ atoms/sec, using revised cross-sections and showing that most of the EUV emission observed by Voyager came from solar UV and photoelectrons and not by magnetospheric electron impact dissociation of N_2 gas. The main reason for this decrease was Strobel et al.'s placement, similar to Hartle et al. (1982), of the ionopause at R_i ~ 4400 km with the exobase being located at R_{exo} ~ 4000 km. Because the scale height (~ 70 km) is much less than 400 km, the magnetospheric plasma electrons in this model did not have direct access to Titan's atmosphere and could only reach the exobase via curvature drift. Furthermore, because the Alfven conductance is much less than the ionospheric conductance, the magnetospheric plasma could not penetrate the ionopause and reach the exobase or lower altitudes. The key to the true estimate of the source term is the actual location of the ionopause relative to the exobase.

Ip (1992) did a more in depth analysis of the magnetospheric interaction issues regarding the ejection of fast neutrals and formation of a Titan nitrogen torus. In this model he estimated an energy spectrum of the fast nitrogen atoms and developed a Monte Carlo description of the torus, which included the collisional transport of the atomic fragments through Titan's atmosphere. Ip stated that the primary reactions responsible for the ejection of fast neutrals (N^*) were the following:

$$N_2 + e \rightarrow N_2^+ + 2e \quad (1)$$

$$N_2 + e \rightarrow N^+ + N^* + 2e \quad (2)$$

$$N_2 + e \rightarrow N^* + N^* + e \quad (3)$$

He then argued, using his earlier ionospheric model (Ip, 1990), that the dominant ion within the ionosphere could be N_2^+ with $N_e \sim 3x10^3$ cm^{-3} and that this peak density could be located near the exobase at R_{exo} ~ 4000 km within a scale height H ~ 70 km; this ionopause height is considerably less than that estimated by Strobel et al. (1992). Ip's model therefore allowed magnetospheric plasma electrons to have access to Titan's upper atmosphere. Below the exobase collisions are important and it will be more difficult for fast neutrals to escape from Titan. The electron dissociation of N_2^+ can produce N atoms with energies greater than the escape energy (0.3eV) due to the excess energy released, $\Delta E = 1.75$ eV. From this mechanism alone the source term is $S_N \sim 2x10^{25}$ atoms/sec. For reaction 2 the launch energies for fast neutrals vary between 0.25 eV and 4 eV. Ip (1992) argued that the bite-out in magnetospheric electrons for E>700 eV reported by Hartle et al. (1982), implies that magnetospheric electrons, via curvature drift, penetrate down to

the exobase. He then said that reaction 3 will tend to dominate with $\Delta E \approx 0.35$ eV (see McElroy et al. (1972) and Rees (1989)), so that the ejection energies are low. Ip (1992) noted that Barbosa and Eviatar (1986) and Barbosa (1987) favor reaction 3. Ip (1992) points out that the vertical distributions of the magnetospheric plasma, ionospheric plasma and extended neutral atmosphere of Titan are complex in the vicinity of the exobase and that modeling the ejection of fast neutrals is very uncertain. The energy spectrum of fast neutrals is also very uncertain. Ip (1992) used a source term $S_N \sim 7x10^{25}$ atoms/sec and had peak densities between [N] = 3-20 atoms/cm^3 at Titan's L shell for which he primarily used reaction 2. On adding reaction 3 he found an additional peak density of 5-50 atoms/cm^3 at Titan's L shell. Since charge exchange is the dominant loss mechanism, the lower range of neutral densities applies when one uses the shorter N atom lifetime $\tau \sim 3x10^7$ seconds from interaction with ambient magnetospheric N^+ within Titan's nitrogen torus versus a longer lifetime $\tau \sim 3x10^8$ seconds when the ambient ion is O^+. Here, we note that although the charge exchange process does not change the number of ions in the plasma, it does replace a more abundant cold ambient ion with a hot keV N^+ ion. The net result is an increase in the plasma energy density and increase in plasma $\beta \sim 11$ (see Neubauer et al., 1984).

Lammer and Bauer (1993) included the impact of magnetospheric N^+ onto Titan's upper atmosphere and the corresponding sputtering of fast neutrals such as N and N_2. They predicted that sputtering was more important mechanism than magnetospheric electron impact dissociation of N_2 and photo-dissociation of N_2 for production of fast neutrals at the exobase. See Johnson (1994) for details about the physics of atmospheric sputtering. This mechanism can be important since the ion gyro-radii are much larger than an atmospheric scale height and the ions have direct access to the atmosphere below the exobase even if the ionopause is 400 km above the exobase in height. However, the model by Lammer and Bauer (1993) ignored collisions below the exobase, and thereby over-estimated the magnitude of the source of fast neutrals for the Titan nitrogen torus. The sputtering mechanism is supported by the observations reported by Hartle et al. (1982), since only ionospheric ions and no hot ions were observed within Titan's wake.

Shematovich et al. (2001) showed the sputtering estimate by Lammer and Bauer (1993) was much too large. The net source rate is $S_N \sim 3x10^{25}$ atoms/sec considering atmospheric sputtering by the rotating plasma ions and magnetospheric electron impact dissociation and photo-dissociation contributions to the ejection of fast nitrogen atoms. The sputtering mechanism can produce very energetic fast neutrals for which the mean escape energy is 2.21 eV to 6.95 eV, which is significantly greater than that produced by magnetospheric electron impact dissociation of N_2 (i.e., $\Delta E \sim 0.25$ eV to 4.0 eV) or photo-dissociation of N_2 (i.e.,$\Delta E \sim 1.43$ eV). However, they found that the dissociation of N_2 by solar EUV photons and corresponding flux of photoelectrons dominated over the sputtering mechanism. In these estimates the slowing of the plasma and the pick-up of heavy ions were ignored. Using estimates of these effects, Shematovich et al. (2003) found that sputtering is competitive with photo-dissociation for producing escaping N atoms and dominates the production of escaping N_2 molecules. A combined source strength $S_N \sim 4.5x10^{25}$ N/sec was given. These calculations used the upstream plasma properties defined by the hybrid model of the Titan interaction with Saturn's

magnetosphere by Brecht et al. (2000), which provided a more realistic description of the interaction. The variation in source strength as described above, depending on the model used, underscores the difficulty in estimating the flux of escaping fast nitrogen atoms and molecules from Titan's upper atmosphere and their corresponding contribution to Titan's nitrogen torus. Therefore, we assign an order of magnitude uncertainty to S_N.

Cravens et al. (1997), using chemistry initiated by photo and electron impact ionization and dissociation without sputtering estimated an upper limit for the source term $S_N \sim 2.5 \times 10^{25}$ atoms/sec of fast N atoms for the Titan nitrogen torus. They also considered other fast atoms and molecules ejected by this mechanism. Here the chemistry would have a carbon contribution.

In addition to the atomic nitrogen torus discussed above, there is the well known atomic hydrogen torus originally detected by McDonough and Brice (1973) with mean density [H] ~ 20 atoms/cm^3 (see also Broadfoot et al., 1981). Shemansky and Hall (1992) have shown that this hydrogen cloud permeates throughout the Saturn system and is not just confined to a torus centered on Titan's orbital position. The hydrogen torus is of similar extent as the nitrogen torus with the added advantage that it has been observed via the strong Lyman alpha emissions, while the nitrogen torus has not yet been detected. The UVIS instrument on Cassini (Esposito et al., 2003) is not expected to detect this nitrogen torus (D. E. Shemansky, private communication, 2004). The pickup energies for the H^+ ions are less than 100 eV and cannot explain the observation of keV ions in the outer magnetosphere as reported by Lazarus and McNutt (1983) and Eviatar et al. (1983) or provide the necessary power for the observed Saturn aurora (Sandel and Broadfoot, 1981). The Cassini Plasma Spectrometer (CAPS) (Young et al., 2003), will be able to measure these pickup ions and their composition throughout Saturn's magnetosphere.

A potentially important source of keV ions within Saturn's outer magnetosphere is the solar wind for which the composition is mainly protons and alpha particles. These ions already have keV energies and can be further energized within Saturn's magnetosphere where the cross-tail potential is ~ 50 kV. Note, that the solar wind was originally considered by Sandel and Broadfoot (1981) as the energy source for Saturn's aurora. In this paper we will consider the relative strengths of the solar wind source and the nitrogen torus and how they compare with Voyager observations. We will consider the leakage of solar wind ions into Saturn's magnetosphere via reconnection at the low latitude boundary layer (Tsurutani et al., 2001,2003), polar cusp and magnetopause and the role that sub-storms at Saturn might play in this process. Tsurutani et al. (2003) presented evidence for the Earth that reconnection in the boundary layer changes the wave spectrum and intensity and that the boundary layer is magnetically connected to the aurora. One would expect Saturn to have a boundary layer similar to that for Earth and Jupiter (see Tsurutani et al., 2001). In the case of a solar wind source the co-rotational electric field may dominate the convection electric field within Saturn's outer magnetosphere and prevent penetration of solar wind ions into Saturn's inner magnetosphere. Here we note that the Kelvin-Helmholtz instability at the dawn magnetopause (see, Goertz, 1983) may provide an important leakage of solar wind ions across the magnetopause into Saturn's magnetosphere. Magnetic field reconnection may

be affected by occasional movement of the magnetopause across the orbit of Titan and its torus in response to variations in solar wind pressure. Solar wind ions can undergo charge exchange in the neutral torus and gain enhanced access as fast neutrals. This same process will produce ~ 50 keV N^+ pickup ions. Like the solar wind, these ions can re-enter the magnetosphere and contribute to the energetic particle population in the outer magnetosphere. We also consider the possible enrichment of nitrogen ions relative to protons as both diffuse radially inward from the Titan torus and populate Saturn's inner magnetosphere where heavy ions have been reported to dominate the energetic ion population (Krimigis et al., 1983). As the suprathermal nitrogen ions diffuse radially inward from the Titan torus with conservation of the first and second adiabatic invariants these ions attain energies E ~ 100 keV at Dione's McIlwain L shell and E ~ 400 keV at Enceladus' L shell. Other energization processes, such as substorms arising from inward convection of magnetotail plasma (Vasyliunas, 1970 and Macllwain, 1974) and acceleration by ELF/VLF waves (Summers et al. 1998), which are known to generate relativistic electrons within the Earth's magnetosphere are possibilities.

The outline of the remainder of this paper is as follows: 1.) The Nitrogen Titan Torus, 2.) Voyager Ion Data at the Titan Torus, 3.) Compare Relative Strength of Different Sources for Suprathermal Ions within Saturn's Outer Magnetosphere, 4.) Enrichment of N^+ Ions Relative to Protons within Saturn's Inner Magnetosphere, 5.) Voyager Ion Data at Dione's L Shell, 6.) Ion Deposition Rates and Radiolysis as a Function of Depth for Dione's Surface, 7.) Present laboratory absorbance spectra based on energetic ion driven radiolysis with nitrogen as an important constituent in the ice, and 8.) Summary and Conclusions.

2.0 THE NITROGEN TITAN TORUS

Using the most recent estimates of the sputtering of Titan's atmosphere by UV photons and by the magnetospheric ions and electrons (Shematovich et al 2003) and the corresponding energy distribution of the ejecta, a Monte Carlo calculation of Titan's neutral torus was carried out. Although both N_2 and N are ejected, we assume in this model that nitrogen is fully dissociated for simplicity. The effect of the molecular nitrogen is being described separately (see Smith et al., 2004). In Figure 1, a Monte Carlo calculation is shown of the atomic nitrogen torus and includes the gravitational fields of both Saturn and Titan as well as a neutral lifetime against ionization of $\tau_{N0} \sim 3 \times 10^7$ sec (Barbosa, 1987). There is a concentration of atoms centered on Titan's L shell with peak densities ~ 4 atoms/cm^3, mean radial extent from 8 R_S and 25 R_S, vertical thickness of ± 2 R_S, and density concentrated at the equatorial plane, but some neutral trajectories extend all the way into Saturn's inner magnetosphere. The figure shows the neutral density as a function of radial distance and latitude. This will be used in the next section along with the observed suprathermal ion densities derived from the Voyager plasma data and corresponding radial diffusion resident time scales. This calculation is an improvement of that presented by Barbosa (1987) since it uses a realistic expression for the energy spectrum of ejected nitrogen atoms at Titan's exobase, displays their true radial and latitudinal dependence and includes a more realistic description of the gravitational field of the system. As expected, the solutions show a concentration of N atoms at Titan. The

model calculations are run, until a steady state is achieved. The solutions are presented in 2D using a grid size of 320x300 cells with Titan fixed relative to Saturn in longitude, although the calculations were done in 3D with Titan orbiting around Saturn. Calculations by Smith et al. (2004) do consider the variation of the ionization time scale as a function of radial distance and latitude. Here, the effects of the magnetopause boundary and bow shock also need to be considered for a truly 3D calculation. As noted above we estimate a torus, which is ½ the thickness of that estimated by Barbosa (1987) with a corresponding reduction of torus volume by factor of 4, giving an average neutral density of [N] ~ 3-4 atoms/cm^3.

Cravens et al. (1997) studied the possibility of other molecular species being ejected from Titan's exobase and contributing to the neutral torus and ion source. Future Monte Carlo calculations should include these species since their source strength may be as high as S_M ~ 10^{25} molecules/s. These predictions will then be able to be compared with the ion formation rates to be measured by CAPS during the Cassini tour of the Saturn system.

3.0 VOYAGER ION DATA AT TITAN TORUS

In this section we will consider the Voyager observations of the plasma and energetic particle populations within the Titan torus region using the Voyager Plasma Science Experiment (PLS) observations (see Bridge et al. (1977)) and Low Energy Charged Particle Experiment (LECP) observations (see Krimigis et al., 1977). These results will then be used with source rates presented in the previous section to estimate resident time scales of the ions within the torus region. We will also compare the two data sets together as a function of intensity versus energy and determine what assumed composition gives the best comparison of the two data sets across the energy gap separating the two data sets. PLS was able to discriminate between protons and nitrogen suprathermal ions because of Mach number effects, but for the LECP instrument this is more difficult. Here, we do note that Maclennan et al. (1982) did an analysis of Voyager 1 LECP data centered on the Titan encounter period. They were able to estimate flow speeds ~ 200 km/s, consistent with Hartle et al. (1982), assuming protons and observed a slow down of the flow centered on Titan's orbit. Therefore, this analysis would favor a composition dominated by protons for E > 30 keV. We will also compare the temperatures of the suprathermal ions measured by PLS and the estimated pickup energies of the assumed ion species.

In Figure 2, we show a three-component Maxwellian fit to the Voyager 1 PLS data, for which the suprathermal component is assumed to be N^+. These measurements were made near the equatorial plane in the Titan torus and would also provide a good fit for O^+ as the suprathermal component, but not for H^+. The density for the suprathermal component is [N^+] = 0.12 ions/cm^3, with flow speed of 120 km/s and temperature T_{N+} = 3.9 keV. This temperature is close to the pickup energy for N^+ with a flow speed of 120 km/s. The results reported by Richardson (1986) showed that on average the azimuthal speed of the thermal ions saturated at around 60 km/sec due to mass loading as originally predicted for Jupiter's magnetosphere by Hill (1980). Under these circumstances the maximum pickup energies would be confined below 800 eV for N^+ pickup ions. After analyzing the

ambient ions in the vicinity of Titan, Hartle et al. (1982) reported that the plasma was hot and that flow speeds were between 80 km/sec and 150 km/sec with a mean speed of about 120 km/sec. In the example shown above the azimuthal speed is around 120 km/sec. In this outer region we have a mixture of flux tubes with cold plasma and hot plasma and just hot plasma. The analysis by Richardson (1986) was primarily confined to plasma where cold plasma was present, densities higher and thus mass loading greater. So, we would argue that the results by Richardson (1986) had a selection effect for which it would tend to analyze those flux tubes with denser cold plasma, correspondingly greater mass loading and thus lower azimuthal speeds. For those flux tubes with azimuthal speeds of 120 km/sec, the maximum pickup energy for N^+ could be as high as 4 keV. The density estimate $[N^+] \sim 0.12$ ions/cm^3 for the suprathermal component is considered an upper estimate and that a more typical value $[N^+] \sim 0.05$ ions/cm^3 is more appropriate. Using this number, a neutral density $[N] \approx 4$ atoms/cm^3 from Figure 1, and ionization time $\tau_{N0} \sim 3 \times 10^7$ seconds, this gives an N^+ ion residence time,

$$\tau_R \approx ([N^+]/[N])\tau_{N0} \approx 4.5 \times 10^5 \text{ seconds} \approx 5.25 \text{ days}$$

This expression equates the ion production rate for keV N^+ formed in the neutral torus and the loss of keV N^+ via radial transport. We expect radial transport via centrifugally driven transport to dominate over other potential loss processes for the ions measured by PLS. Near Dione the above estimate is comparable to the maximum diffusive transport time for O^+ ions from the OH neutral cloud model of Richardson et al. (1998), who also noted that centrifugal transport effects should increase transport rates beyond 12 R_S, so this value is probably an upper limit ruling out the large torus volume estimated by Barbosa (1987). If protons from the hydrogen torus (Shemansky and Hall, 1992) were assumed for the suprathermal ions then the estimated resident time scale would be shorter as expected, but the energy spectrum is inconsistent with their pickup energies, which is ~ 100 eV. As discussed below, the source term for solar wind protons could be competitive with nitrogen ions. As noted above, protons provide a poorer fit to the suprathermal ion component in the PLS spectrum shown in Figure 2. It is important to note that pickup ions initially form ring distributions (see Sittler et al. (2004a)) and are expected to pitch angle scatter into shell distributions (Vasyliunas and Siscoe, 1976a). In Figure 3 we show a Voyager 2 PLS spectrum near Titan's L shell, but at high latitude. Here, we see no evidence of a suprathermal ion component. If steady state is assumed this indicates that the suprathermal ions are confined near the equatorial plane, which is consistent with our nitrogen torus calculations, showing the N atoms confined within 2 R_S of the equatorial plane. These observations also indicate that the pickup ions retain their initially large perpendicular energy relative to the planetary magnetic field (i.e., $T_\perp / T_{ll} >> 1$) and that formation of shell distributions from ion scattering is not dominant. Sittler et al. (2004b) from a re-analysis of the Voyager 1 Titan encounter PLS data showed that finite gyro-radius effects were important and that the hot keV ion component had to be a heavy ion such as N^+ with ion gyro-radius $r_g \sim 5600$ km.

Compared to the radial diffusion coefficient $D_{LL} \sim 5 \times 10^{-7}$ R_S^2/s used for Richardson et al.'s OH model, Paranicas and Cheng (1997) used ~ 10^{-7} R_S^2/s to fit measured phase space density profiles, assumed to be for ~ 100-keV O^+ from Voyager LECP

measurements, in the macrosignature region of Enceladus. However, there is great uncertainty in using moon absorption signatures of energetic particles (e.g., Paranicas et al., 1997) to determine transport rates without quantitative estimates for injection rates at these energies from distributed sources such as E-ring grain sputtering (Jurac et al., 2001a,b). Apparent radial dependence of radial diffusion rates for loss-less diffusion can arise from radial variation of source and loss rates. This was strongly suggested by the phase space density analysis for LECP ion and electron data of Armstrong et al. (1983), who derived diffusion rates increasing towards Saturn for loss-less diffusion and highly contrary to known diffusion models, all with positive radial gradients in D_{LL}. Diffusion rates may also be strongly dependent on energy and momentum. Cooper (1983) and Randall (1994) respectively derived diffusion rates for high energy protons and electrons, both explicity using models for sources of these particles from cosmic ray albedo neutron decay (CRAND) in the inner magnetosphere, in the range $D_{LL} \sim 1 - 3 \times 10^{-10}$ R_S^2/s near Enceladus, three orders of magnitude less than the results from Voyager PLS and LECP. Finally, apparently high diffusion rates can be derived from moon microsignatures (e.g., Carbary et al., 1983; Paranicas and Cheng, 1997) on the assumption that electron and ion drift shells have longitudinal symmetry, but Cooper et al. (1998) has demonstrated that this assumption can be dramatically violated for keV-MeV electrons due to effects of global electric fields in the magnetosphere. In the most extreme cases, for electron energies near longitudinal drift resonance where corotational motion is cancelled by equal and opposite gradient curvature drift, the electron drift shells close in banana-shaped configurations on the dusk side of Saturn and do not extend fully around to the dawn side. Dawn-dusk asymmetries in intensities and phase space densities of keV-MeV ions (Krimigis et al., 1983) and electrons (Maurice et al., 1996) generally suggest that longitudinal symmetry of global transport is a poor assumption. These issues will have important implications when we discuss various source and loss mechanisms for the charged particle populations in sections 4 and 5.

In Figure 4 we show a combined plot of the PLS and LECP ion data in the Titan torus region where N^+ ions are assumed both for the PLS suprathermal component and for the LECP data. We used the calibration data for heavy ions presented in Krimigis et al. (1981) paper for Jupiter's magnetosphere for our analysis of the LECP data. For these calculations we used raw count rate data, which is independent of composition and removed data from one directional sector, sector one, which is contaminated from sunlight entering the sensor. Background corrections from energetic electrons in this region are estimated to be negligible, for both instruments but are important in the inner magnetosphere (Paranicas et al., 1997). We used 30-minute averages. We have also super-imposed the PLS-LECP electron intensities from Maurice et al. (1996) for both Voyager 1 and 2. The PLS ion data has been converted from instrument currents to particle intensities.

When one compares the energy spectrum across the energy gap between the two instruments, the comparison is very good. If we assume that protons dominate the suprathermal ions the comparison is not as good. For example, in data presented in Krimigis et al. (1983), for which protons are assumed, the LECP spectrum is shifted towards lower energies and the comparison between PLS and LECP is correspondingly

not satisfactory. Furthermore, if one uses the 500 keV proton intensities measured by the LECP channel 32 as reported by Krimigis et al. (1983), they are only 10% of those estimated here for N^+. However, protons may very well dominate the spectrum at high energies if the source of these ions is the solar wind and there is efficient access into Saturn's outer magnetosphere. Here we refer one to the classical papers by McIlwain (1974) and Vasyliunas (1970, 1975, 1976b). Magnetospheric convection can be an important process for accelerating solar wind protons and alphas within Saturn's magnetosphere similar to that for the Earth's magnetosphere. But, as discussed in the next section the defining parameter is the ratio of the convection electric field relative to the rotational electric field within Saturn's outer magnetosphere. As previously noted, the analysis by Maclennon et al. (1982) favored a composition dominated by protons for E > 30 keV within the Titan torus. Therefore, the composition of these energetic ions in the outer magnetosphere cannot be determined with certainty.

If the high energy component observed by LECP is dominated with N^+ ions, then these high energies could be the result of turbulence in the outer magnetosphere acting on pickup N^+ ions as the seed population. For example, the N^+ ions could satisfy a bounce resonant interaction with ULF waves in the outer magnetosphere (see Schultz and Lanzerotti, 1973). The Voyager magnetometer data does show the presence of turbulence in the outer magnetosphere (Lepping et al., 1986, 2004), which could indicate VLF or ULF waves or compression-expansion episodes of the magnetosphere caused by the solar wind interaction (Southward and Hughes, 1983; Hughes, 1994; Anderson, 1994; Sibeck, 1994; Mathie and Mann, 2000). More comprehensive magnetometer data for wave analysis will become available from the Cassini orbiter at Saturn after orbital insertion on July 1, 2004. It is also important to note that the ion pressure in the LECP data near Titan's orbit is about 50% of that below 10 keV, although a majority of the ion density is below 10 keV. The total ion pressure is ~ 0.2 nPa, the total electron pressure is ~ 0.01 nPa and the magnetic field pressure is ~ 0.01 nPa. Therefore, the plasma beta is estimated to be $\beta >> 1$, which means that a vacuum approximation for Saturn's magnetosphere is not appropriate, similar to that for Jupiter. This equipartition of energy between the low energy plasma and hot plasma is similar to that observed for the electron component of Saturn's magnetosphere as reported by Maurice et al. (1996).

4.0 COMPARE RELATIVE STRENGTH OF DIFFERENT SOURCES FOR IONS WITHIN SATURN'S MAGNETOSPHERE

4.1 Solar Wind Source

A solar wind source (i.e., protons and alphas) within Saturn's outer magnetosphere can provide keV and even hotter protons. The source strength for solar wind protons can be roughly estimated using the following expression

$$S_{SW} \approx (N_{SW}V_{SW})(\pi(R_M/2)^2)(1/2)\varepsilon$$

The ½ factor is used since half the time the solar wind B_Z will point northward for reconnection on the front side magnetosphere and solar wind entry into the

magnetosphere and southward for a closed magnetosphere with no entry into the magnetosphere. At Saturn N_{SW} = 0.05 ions/cm^3, V_{SW} = 400 km/s, R_M = 20 R_S and ε = efficiency for solar wind entry into Saturn's magnetosphere. At Earth ε ≈ 0.05 and the efficiency goes like $1/M_A$ (M_A = Alfven Mach number in the solar wind = V_{SW}/V_A ≈ 10) (see Slavin and Holzer, 1979) which reduces ε by 1.5 relative to that at Earth, so ε ≈ 3 %. For this value of ε we get $S_{SW} \approx 4x10^{26}$ ions/sec. In addition, $E_{cor} >> E_{conv}$ at Saturn, so this efficiency could be lowered by an additional factor β, where $0.01 < \beta < 1.0$. This parameter is essentially unknown and probably will require measurements by CAPS during the Cassini tour of Saturn's magnetosphere. If we assume β ~ 0.1, then we get S_{SW} ~ $4x10^{25}$ ions/sec.

4.2 Titan Torus Source

The source strength for the nitrogen torus is $S_{N+} \approx (4.25 \times 10^{25}$ ions/sec)(2/3) = 2.8×10^{25} ions/sec (Note, the factor of 2/3 is used since part of the neutral torus can extend into the magnetosheath). Therefore, the source strength of the suprathermal keV N^+ ions is about the same as that for solar wind keV protons. So, the estimated Titan nitrogen torus and solar wind sources in the outer magnetosphere for hot suprathermal ions are about equal. Titan's hydrogen torus is not considered since pickup energies are about 100 eV and therefore do not correspond to the suprathermal ions observed by PLS within the Titan torus region. In the case when the magnetopause is pushed inside of Titan's L shell, charge exchange reactions will produce ~ 50-100 keV N^+ and ~ 4 keV H^+ pickup ions (i.e., V_{SH} ~ 400 km/s) within the magnetosheath and energetic atomic hydrogen atoms, E_{H*} ~ 1 keV, that would be ejected from the Saturn system. The pickup N^+ ions would tend to be convected away by the magnetosheath flow, but some could re-enter the magnetosphere, similar to solar wind protons, with very high injection energies E_{N*} ~ 50-100 keV and higher since the polar cap potential could exceed 400 kV (see later discussions). The importance of this source of energetic N^+ ions and H^+ is difficult to estimate, but could be as high as $S_{N*+} \sim 3x10^{23}$ ions/sec for N^+ and $S_{H+} \sim 4x10^{24}$ ions/s for H^+ (i.e., density of hydrogen cloud N_H ~ 20 atoms/cm^3). The N^+ ions could contribute to the energetic ions observed by LECP, while the H^+ ions could contribute to the suprathermals observed by PLS within Saturn's outer magnetosphere. This relatively large injection of energetic particles would only occur during the passage of compression regions and coronal mass ejections (CMEs). Although, temporal, they could contribute to the more permanent energetic populations within Saturn's magnetosphere. Since, part of the torus is always in the magnetosheath plasma regime, a smaller energetic source of N^+ ions will always be entering Saturn's outer magnetosphere and contribute to its energetic population.

4.3 Sub-Storms and Charged Particle Energization

It is important to consider the possibility of sub-storms at Saturn and the consequences they will have on the charged particle populations and their energetics within Saturn's magnetosphere. During the growth phase of substorms at Saturn we expect to have time scales $\tau_G \sim (2\pi B_T R_M)/(B_{SW} V_{SW}) \approx 2$ days (B_T = 3 nT, B_{SW} = 0.5 nT, R_M = 20 R_S, V_{SW} = 400 km/s). In the case of the Earth, τ_G ~ 2.5 hours, while for Mercury we expect τ_G ~ 1-2

minutes (Siscoe et al., 1975). We estimate the time scale for an injection event after sub-storm onset to be $\tau_I \geq 2$ hours when neglecting line tying effects (i.e., this time scale could be longer), while for Earth the injection time scales $\tau_I \sim 40$ minutes or less (McPherron, 1997; McPherron et al., 1986). As estimated above, the polar cap potential drop $\Delta\Phi_{PC} \approx (V_{SW}B_{SW})(2R_M)\eta \approx 48$ kV for which we set $\eta \approx 0.1$ (Tsurutani and Lakhina, 1997). This large potential drop across the polar cap can energize solar wind ions to very large energies via the return flow from the magnetotail (see Vasyliunas, 1970; Vasyliunas, 1975; Vasyliunas, 1976). Using the poynting flux as described by Siscoe et al. (1975), the total input power is $W \sim R_M\Delta\Phi_{PC}B_T/\mu_0 \approx 1.4x10^{11}$ watts, very close to the EUV aurora power reported by Broadfoot and Sandel (1981) of $\sim 2x10^{11}$ watts. If we use a solar wind source at the magnetopause or boundary layer of $S_{SW} \sim 4x10^{26}$ ions/s and use a power input due to convection of $W \sim 1.4x10^{11}$ watts, we get a mean energy of solar wind protons of $E_P \sim 2.5$ keV. This estimate is comparable to their mean energy of $E_P \sim 1$ keV in the solar wind. If, we use the lower estimate for the solar wind source, then the protons will be energized to $E_P \sim 25$ keV, which is comparable to the polar cap potential. At the orbit of Titan the rotational electric field $E_{rot} \approx V_{rot}B_{Titan} \sim 300$-$600$ μV/meter ($V_{rot} \sim 60$-120 km/s, $B_{Titan} \approx 5$ nT), while the convection electric field $E_{conv} \approx (V_{SW}B_{SW})\eta \sim 20$ μV/meter << E_{cor} as previously argued. The parameter η is highly uncertain. During the passage of a compression region and if we assume a jump in B and density by a factor of 4, (Smith et al., 1980), then the convection electric field could increase to $E_{conv} \sim 160$ μV/meter and start to be competitive with the rotational electric field. Futhermore, the merging rate efficiency at the magnetopause is inversely proportional to the Alfven Mach number (Slavin and Holzer, 1979), which could decrease by a factor of two within a compression region, and increase $\eta \sim 0.2$. Therefore, the number of particles entering the magnetosphere could increase by a factor of 16 (i.e., β factor also increased by factor of 2), the polar cap potential to $\Delta\Phi_{PC} \sim 400$ kV (i.e., charged particle energization) and the input power to $W \sim 1.1x10^{12}$ watts and resulting in auroral brightening. The presence of boundary layers at all planetary magnetospheres are expected to be present, for which the low latitude boundary layer (LLBL) plays a most critical role with regard to magnetospheric convection and substorm phenomena (Tsurutani et al., 2001; Sonnerup and Siebert, 2003). The LLBL can also be an important source for ELF/VLF plasma waves within the outer magnetosphere and result in crossfield diffusion (i.e., turbulent electric fields) of ions and electrons into the magnetosphere (i.e., boundary layer thickness) where they can be further energized via field aligned electric fields and corresponding auroral brightnings (Tsurutani et al., 2003). Once these particles have entered the magnetosphere, they can be further energized by magnetospheric convection processes. One of the primary objectives of the Cassini mission is to provide a more accurate estimate of the parameter η, related to the ε parameter noted above, and to search for the presence of a boundary layer during magnetopause crossings.

5.0 ENRICHMENT OF NITROGEN IONS RELATIVE TO PROTONS WITHIN SATURN'S INNER MAGNETOSPHERE

5.1 Sources

Using LECP ion data Armstrong et al. (1983) showed measured phase space densities suggesting that the source of the sub-MeV energetic ions above 10 keV was in the outer magnetosphere and that the inner magnetosphere was populated by these ions via inward radial diffusion. The conventional adiabatic diffusion theory (e.g., Schulz and Lanzerotti, 1974) was assumed in which the first and second adiabatic invariants were conserved with radial diffusion resulting from violation of the third adiabatic invariant. The ion composition for modeling was assumed to be protons but could have been heavier ions (O^+ or N^+) since neither sources nor losses dependent on ion species were included. The phase space density profiles showed losses occurring around Rhea's L shell and inward. A major problem with this result, however, was that simple models for loss-less inward diffusion could not be fitted with realistic diffusion coefficients to the data. The fitted coefficients had negative radial gradients in contrast to the usual positive-gradient form $D_{LL} \sim L^n$ for n = 3 to 10. The most recent LECP analysis by Paranicas et al. (1997), including electron background corrections for the ion channels in the inner magnetosphere, now requires inner sources for ions up to 4 MeV to account for local minima in phase space densities, although fits for radial distributions of sources, losses, and diffusion coefficients have not been included in this work.

Another indication of an outer source was suggested by the shape of the LECP ion energy distribution as reported by Armstrong and Krimigis (1982). In the inner magnetosphere, inwards of Enceledus, this distribution was apparently composed of two separate parts: (1) a soft spectrum rising in differential flux towards lower energies below a few MeV, and (2) a hard spectrum above 10 MeV with a flux maximum around 100 MeV. The latter was easily accounted for by a distributed source of high energy protons from cosmic ray neutron albedo decay (CRAND), as first proposed by Fillius et al. (1980) from Pioneer 11 data and later modeled in detail for Pioneer 11 (Fillius and McIlwain,1980; Van Allen et al., 1980; Cooper, 1983) and Voyager 2 (Schardt and McDonald, 1983) proton measurements. Randall (1994) later also found evidence from Pioneer 11 electron data for an inner source of energetic electrons, likely from CRAND.

But the species and origin of the soft low-energy component remains elusive and could be from some combination of internal distributed sources, e.g. E-ring grain sputtering for water group ions at lower energies (Jurac et al., 2001), and inward diffusion from the outer magnetosphere for more energetic ions. Here we suggest that the latter are dominated by N^+ ions diffusing inward from the Titan torus. In order to distinguish the N^+ source from outer magnetosphere sources for H^+, e.g. from abundant hydrocarbons in Titan's atmosphere and from the solar wind, we now consider the relative effects of inward transport on N^+ and H^+ ions from losses including moon sweeping, E-ring absorption, and wave-particle interactions.

5.2 Icy Satellite L Shell Sweeping

In Figure 5, we show the loss of ions via satellite sweeping at Rhea's L shell, as calculated by Paranicas and Cheng (1997), for an assumed composition of protons or nitrogen ions at an energy E ~ 100 keV. These calculations were performed for radial diffusion transport time scales $\tau_D \sim 1 - 100$ days, for which the radial diffusion

coefficient D_{LL} is assumed to vary as L^3. For fast radial transport ($\tau_D \sim 1$ day) neither ion experiences significant losses, hence, no significant enrichment of N^+ ions relative to protons occurs. For intermediate radial transport ~ 10 days, the losses are significant for protons but about a factor of 10 less for nitrogen ions. Under these conditions satellite sweeping will tend to enrich nitrogen ions within Saturn's inner magnetosphere relative to that for protons. In the case of slow radial diffusion ($\tau_D \sim 100$ days), both species experienced large losses and no enrichment for N^+ ions occurs relative to protons.

The longitudinal speed of gradient-curvature drift motion (Thomsen and Van Allen, 1980) relative to Rhea which orbits around Saturn each 4.75 days, is the same for 100 keV H^+ and N^+. Enrichment of N^+ ions relative to protons for intermediate radial transport time scales can instead be traced to the larger gyro-radius for N^+ ions relative to that of protons and to longer periods for latitudinal bounce motion along the magnetic field lines. At 100 keV the gyro-radius r_g for protons is ~ 1600 km and ~ 5700 km for N^+ ions, while the diameter of Rhea is $2R_{Rhea} = 1528$ km. The N^+ ion speed at 100 keV is about four times slower than for H^+at the same kinetic energy. Thus a proton encountering Rhea is much more likely to impact the surface during gyromotion, and also moves back towards the moon four times more quickly during bounce motion. The result is that N^+ can 'leap-frog' more easily than H^+ past Rhea during each longitudinal drift encounter. Ions will be strongly depleted if the time scale for radial transport across Rhea's ion sweeping corridor of radial width $w_S \sim 2(R_m + 2r_g)$ is longer than the time interval $\tau_E \sim 10$ hours (mostly due to Saturn's rotation for 100 keV ions) of consecutive drift encounters with this moon. This corresponds to a critical diffusion coefficient $D_{LL} \sim w_S^2/4\tau_E$ of $2x10^{-7}$ R_S^2/s for 100-keV protons and $1x10^{-6}$ R_S^2/s for N^+, such that both H^+ and N^+ have significant chances of escaping impact on Rhea via radial diffusion for $D_{LL} \sim 5x10^{-6}$ R_S^2/s extrapolated to that moon's orbit with no energy dependence from the plasma ion transport model of Richardson et al. (1998). If drift shells are significantly distorted from longitudinal symmetry over radial scales $w_D >> w_S$ (e.g. due to time variations in magnetospheric electric fields) then the critical value of D_{LL} increases by a factor $(w_D/w_S)^2$, which is ~ 24 for 100-keV N^+ and ~ 57 for H^+ with $w_D \sim 1$ R_S. Clearly, the 100-keV ion diffusion rates must be far greater than the ~ 10^{-9} R_S^2/s value extrapolated to Rhea's orbit for 100-MeV CRAND protons from the model of Cooper (1983), suggesting that D_{LL} must decrease at least linearly with ion energy E for 100-keV protons to survive traversals across Rhea's orbit where the CRAND protons would be strongly depleted.

5.3 E Ring Absorption

The loss due to dust particles is given by the following expression

$$\tau_{dust} = (3/8)(R/r_0)T_B\cos\alpha/\eta_{opacity}$$

as given by Thomsen and Van Allen (1979), where α = equatorial pitch angle, $\eta_{opacity}$ = E ring opacity, R is the ion range, r_0 is the dust particle radius and T_B is the particles bounce period which varies like 1/v with v = the charged particle's speed. At Enceladus $\eta_{opacity} = 10^{-6}$ and at Rhea's L shell $\eta_{opacity} = 10^{-8}$ (Baum et al., 1981). The particles range in ice R

can be determined using the Stopping Range in Matter (SRIM) data of Ziegler et al. (1985). The dust particle diameter $d = 2r_0 = 1$ micron (Baum et al., 1981), and the average path length through a spherical dust particle is $4r_0/3$.

The respective ranges of 100 keV H^+ and N^+ (see Figure 6) are about 1.7 and 0.5 microns in unit density water ice, but the shorter bounce period and correspondingly higher ring plane crossing rate of protons compensates for the greater range. The range of a 100 keV proton is about 1 micron, so at lower energies protons are depleted relative to N^+ as they diffuse radially inward because of their shorter bounce period. At higher energies N^+ is depleted more than protons. But, because of the E ring's low opacity at Rhea's L shell, the time scale for absorption is $\tau_{dust} \sim 10^8$ seconds (~ 3 years) for protons and even longer for nitrogen ions. Therefore, at Rhea E ring absorption for ions is negligible when compared to reasonable radial diffusion time scales $\tau_D \sim 1 - 100$ days. At Enceladus $\tau_{dust} \sim 10^6$ seconds (~ 10 days) and E ring absorption becomes more important for ions. In the case of electrons the absorption time scales are 43 times shorter, thus more important for keV electrons whose range is less than a dust particle's diameter $d \sim 1$ micron. At MeV energies the loss by dust particle absorption for electrons is small $\tau_{dust} \sim 10^7$ seconds at Rhea's L shell. In conclusion, we can neglect E ring absorption effects on ions outside Dione's L shell.

5.4 Precipitation by Waves

As discussed in Schultz and Lanzerotti (1974) the pitch angle scattering rates of ions by various wave modes are inversely proportional to ion mass m and kinetic energy E, so that protons are depleted more effectively than N^+ at the same energy. Therefore, this mechanism could also enrich N^+ ions relative to protons within Saturn's inner magnetosphere as the ions diffuse radially inward. The various wave modes one might consider are ULF waves, VLF waves, bounce resonant wave-particle interactions and cyclotron resonance wave-particle interactions (Southwood and Hughes, 1983; Hughes, 1994; Anderson, 1994; Sibeck, 1994). In order to study these various modes within Saturn's magnetosphere we look at the Voyager and Pioneer 11 magnetometer data and infer the wave power as a function of frequency. For example, within the Titan torus there is a lot of power at low frequencies (i.e., 7 mHz) relative to higher frequencies (i.e., 100 mHz) so that the scattering of heavy ions by waves at keV energies may be more important than that for keV protons, but these low frequency waves will also resonate with more energetic protons with $E > 150$ keV. We already know that ion cyclotron waves are important near Dione's L shell and near the equatorial plane (Smith and Tsurutani (1983) and Barbosa (1993)). The analyses of the Pioneer 11 and Voyager magnetometer data for MHD waves in Saturn's outer magnetosphere are incomplete and we only have the results by Lepping et al. (1986, 2004), who used Voyager magnetometer data at $8.5 \leq L \leq 16.9$.

The analysis by Lepping et al. (1986, 2004) showed the presence of MHD waves in the pickup region of the Titan torus, a trend toward lower levels at smaller r where Rhea's L shell resides, and enhanced levels in the vicinity of Dione where ion cyclotron waves (Smith and Tsurutani, 1983, Barbosa, 1993) were observed. In the vicinity of Dione

enhanced levels of pickup ions are also expected from the OH cloud within the inner magnetosphere (Richardson et al., 1998). In Section 6 we show the observation of suprathermal ions by PLS during the Dione ring plane crossing by Voyager 1. These observations are consistent with the presence of pickup water group ions. Waves observed in the vicinity of Rhea are interpreted here to not be locally produced and must propagate from the inner and outer sources. A preliminary analysis of the wave data is presented for ion scattering via ion cyclotron resonance. In Table 1 we summarize our results using the Lepping et al. (1986, 2004) results as the basis for our analysis.

In discussions to follow we consider pickup nitrogen ions or solar wind protons with energies ~ 4 keV within the Titan torus and then trace these particles to the inner magnetosphere by conserving the first and second adiabatic invariants. We also consider those ion species in resonance with the wave spectrum peak, for which pitch angle scattering will be at its maximum value. Furthermore, we assume that the spectral shape of the power spectrum, in a relative sense, will be the same for all periods analyzed by Lepping et al. (1986, 2004). At higher frequencies, away from the spectral peak, the wave amplitudes are near the magnetometers noise level where quantization noise can dominate. Therefore, under these conditions our estimated pitch angle diffusion coefficients are upper estimates. We also assume, within the peak of the wave power spectrum, where compressional modes dominate, that comparable but smaller levels of ion cyclotron waves are also present but masked by the compressional wave components.

In the table we list parameters for protons and nitrogen ions at L shell values covered by the Lepping et al. (1986, 2004) study. The electron densities come from Sittler et al. (1983), Maurice et al. (1996) and Richardson and Sittler (1990). The azimuthal velocities V_R of the flow come from Hartle et al. (1982) and Richardson (1986).

Table 1.

Parameter	Protons			Nitrogen Ions		
L Shell	16.9	15	8.5	16.9	15	8.5
N_e (#/cm^3)	0.1	0.2	2.0	0.1	0.2	2.0
V_R (km/s)	101	90	53	101	90	53
B (nT)	6	10	30.8	6	10	30.8
E_{MAX} (MeV/G)	5.04	1.7	0.21	70.5	23.8	2.94
E_M (MeV/G)	17.8	12.4	4.21	17.8	12.4	4.21
F_{gyro} (mHz)	91.6	153	470	6.54	10.9	33.6
α_L (Deg.)	0.3	0.46	1.63	0.3	0.46	1.63
F_{peak} (mHz)	6.93	8.7	14.03	6.93	8.7	14.03
E_R (MeV/G)	3109	3835	4.7×10^{3}	15.9	19.5	24.1
τ_B (sec)	919	569	165.8	4.8×10^{4}	1.31×10^{4}	8667
$1/\tau_{sd,0}$ (sec^{-1})	3.4×10^{-7}	7.6×10^{-7}	1.5×10^{-5}	6.4×10^{-9}	1.5×10^{-8}	2.8×10^{-7}
$P\Delta f_{MHD}$ (nT^2)	15×10^{-3}	0.163	8.7×10^{-3}	15×10^{-3}	0.163	8.7×10^{-3}
$D_{\alpha\alpha}$ (sec^{-1})	3.7×10^{-6}	1.6×10^{-4}	2.7×10^{-6}	2.6×10^{-7}	1.1×10^{-5}	1.9×10^{-7}

The magnetic field parameters come from Lepping et al. (1986, 2004), E_{MAX} is the maximum pickup energy for the ion in question, $E_M = B^2/(8\pi N_e)$ is the magnetic energy of the ion, f_{gyro} is the gyro-frequency of the ion, α_L is the loss cone angle, f_{peak} is the frequency where the power spectrum is a maximum, $E_R = \left(\frac{\Omega_+}{\omega}\right)^2 E_M$ is the resonance energy of the ion with the wave of frequency ω and Ω_+ is the ion gyro-frequency, $\alpha_L^2 \sim 1/(2L^3)$ (L >> 1) is the ion loss cone squared, $\tau_B \sim 5.4\ R_P\ L/v$ is the ion bounce time, $\tau_{sd,0} = 3.6\ R_P\ L^4/v \approx \tau_B/(3\alpha_L^2)$ is the strong pitch angle scattering time scale, $P\Delta f_{MHD}$ is the wave power centered on the peak in the power spectrum (i.e., but use the amplitude of the wave power when $k_{ll} >> k_\perp$) and

$$D_{\alpha\alpha} \approx \Omega_+ \left(\frac{\delta B}{B}\right)^2 \eta$$

is the pitch angle diffusion coefficient for ion cyclotron wave scattering of ions with gyro-frequency Ω_+, wave amplitude δB and factor η ~ 0.1 (Tsurutani and Lakhina, 1997; Kennel and Petschek, 1966). In the case of weak pitch angle scattering it is appropriate to set the corresponding precipitation loss time scale $\tau_p \sim \tau_{\alpha\alpha} \sim 1/D_{\alpha\alpha}$ (Thorne, 1983). Paonessa and Cheng (1986) estimated upper and lower bounds for the radial diffusion coefficient for L < 9, while our study is confined outside L ~ 9 with regard to wave scattering. For L > 8 they assumed a composition dominated by protons and L < 8 dominated by heavy ions. For their upper limits they used the strong pitch angle limit or the fact that the precipitating ions not produce an aurora for L < 9 using the UV observations reported by Broadfoot et al. (1981) as a constraint. Broadfoot et al. (1981) reported seeing an auroral ring confined between 78° and 81.5° in latitude, which maps to equatorial field lines L > 15. In some cases the strong diffusion limit is larger than the auroral limit and in other cases the auroral limit is larger. We would argue that if the strong diffusion limit were smaller than the auroral limit, then the strong diffusion limit would be the upper bound. For L > 15 the loss cone is so small that we would consider the strong pitch angle scattering limit negligible relative to the radial diffusion coefficient lower limits estimated by Paonessa and Cheng (1986). We also note, that Paonessa and Cheng (1986) considered ion energies between 20 MeV/G and 200 MeV/G which brackets the particle energies being considered in this study. The ion cyclotron waves reported near Dione's L shell by Smith and Tsurutani (1983) and Barbosa (1993) would be in resonance with ~ 1 keV O^+ pickup ions and heavy ambient ions and 125 keV protons. So, with regard to the energetic population within Saturn's inner magnetosphere, these waves are a more important sink for protons than heavy ions. In fact, as will become evident below the waves are generally in resonance with energetic protons and not with energetic nitrogen or oxygen ions. The waves are in resonance with keV heavy ions, but this is because, as we argue in this paper, the keV suprathermal ions are the pickup ion population producing the ion cyclotron waves. Therefore, the waves are a primary sink for energetic protons relative to energetic heavy ions, thus providing an enrichment of energetic heavy ions (i.e., N^+, O^+) relative to energetic protons within Saturn's magnetosphere. One should keep this in mind when considering the following

discussions. We note, that the wave peak is ~ f_{peak} wide (Lepping et al., 1986, 2004), so that the band of resonance energies will be confined to $E_R/2 < E < 4E_R$. Finally, in Lepping et al. (1996, 2004), they used a 4th order polynomial in time to de-trend the data and may have inadvertently removed the ultra low frequency ion cyclotron waves which may have been in resonance with energetic heavy ions.

The relevant time scales due to wave scattering and radial diffusion can be found in Table 1 and Figure 7. In Figure 7 we show horizontal dashed lines of 1 day (blue), 10 days (green) and 100 days (red) for radial diffusion time scales relevant to our previous discussions concerning satellite sweeping losses. We also show in this figure the radial transport time scales as a function of r as determined by Richardson et al. (1998) τ_R ~ 5 days at Dione's L shell (blue line) and section 3.0 of this paper where we derived a time scale τ_R ~ 5.25 days at L ~ 20 (red line). We use vertical lines at r = 4 R_S and r = 20 R_S to indicate the radial range of our analysis. These curves provide a bracket around allowed radial transport time scales as a function of radial distance for Saturn's middle and outer magnetosphere. The figure contains a plot of the strong diffusion time scales for protons (diamonds) and N^+ or O^+ ions (triangles) as a function of radial distance when these ions are at the appropriate energy to be in resonance with observed ion cyclotron waves reported by Lepping et al. (1986; 2004) and Smith and Tsurutani (1980). We show the strong diffusion limit for N^+ or O^+ ions at the energies for which protons are in resonance with the ion cyclotron waves (squares). We show the pitch angle scattering time scales for protons (X) and N^+ or O^+ ions (+) in resonance with the ion cyclotron waves, and the pitch angle scattering time for N^+ ions (blue square) and 'solar wind' protons (red square) born at L ~ 20 and one conserved the 1st and 2nd adiabatic invariants as they diffuse radially inward. Finally, we show the charge exchange time scales for N^+ or O^+ ions (blue *) and protons (red *) who are born at L ~ 20 and diffuse radially inward and conserve the 1st and 2nd adiabatic invariants.

In the outer magnetosphere for L > 15 the strong diffusion limit for protons and N^+ ions, $\tau_{sd,0}$, is greater than the allowed radial transport time scales τ_R and precipitational losses should be small. For smaller radial distances the strong diffusion limit for protons can be less than allowed radial transport times scales, while for N^+ $\tau_{sd,0} < \tau_R$ does not occur until L < 9 at the upper range for τ_R and does not occur until L < 4 for the lower range of τ_R. This says that precipitational losses can be important for energetic protons within the inner magnetosphere, but not important for N^+ ions. When we look at the scattering time scales for energetic protons in resonance with the waves (i.e., with resonance energies E_p ~ 186 keV at L ~ 17 and E_p ~ 384 keV at L ~ 15) their scattering times scales $\tau_{\alpha\alpha} << \tau_{sd,0}$ with $\tau_{\alpha\alpha} \sim \tau_R$ or shorter in the outer magnetosphere, L > 10, so that the energetic protons will become isotropic in pitch angle but precipitational losses will be small. In this limit protons will tend to fill a flux tube at all latitudes. Within the inner magnetosphere at L ~ 8.5 (i.e., with resonance energy E_p ~ 1.45 MeV) for energetic protons $\tau_{\alpha\alpha} > \tau_{sd,0}$ so we are at the weak pitch angle limit but since $\tau_{\alpha\alpha} \sim \tau_R$ precipitational losses are expected to be important. In the case of N^+ ions scattering times scales at L ~ 17 (with resonance energies E_{N+} ~ 1 keV) are long compared to transport times scales (i.e., $\tau_{\alpha\alpha} >> \tau_R$) such that the picked up N^+ ions will retain their large pressure anisotropy (i.e., $T_\perp / T_{ll} >> 1$) and thus remain confined to the equatorial plane. At L ~ 15 (with resonance energy E_{N+} ~

2 keV) the N^+ ions will be in the strong scattering limit, $\tau_{\alpha\alpha} < \tau_R$ and $\tau_{\alpha\alpha} << \tau_{sd,0}$, so that they will tend to be isotropized but precipitational loses will be negligible $\tau_{sd,0} >> \tau_R$. Inside of Rhea's L shell the N^+ ions (i.e., resonance energy $E_{N+} \sim 7.5$ keV) are weakly scattered by the waves with $\tau_{\alpha\alpha} > \tau_R$ and $\tau_{\alpha\alpha} > \tau_{sd,0} > \tau_R$ so that they will tend to retain their pressure anisotropy with minimal precipitational losses.

We will now consider the case of pickup N^+ ions and 'solar wind' protons which are born at L ~20 and diffuse radially inward while preserving the 1st and 2nd adiabatic invariants. Here, their mean energy will vary from E ~ 4 keV at L ~ 20, E ~ 6.5 keV at L ~ 17, E ~ 10 keV at L ~ 15, E ~ 52 keV at L ~ 8.5 and E ~ 128 keV at L ~ 6.3. In all cases, both protons and N^+ ions will not be in resonance with the waves and pitch angle scattering time scales will be considerably smaller (i.e., use power levels only 5% of main peak). In the case of N^+ ions they should retain their large pressure anisotropy $T_\perp/T_{||} >> 1$ throughout Saturn's magnetosphere and be confined to the equatorial plane. In the case of protons the scattering time scales will be larger by the mass ratio (i.e., factor of 14) so that the 'solar wind' protons could be isotropized by the waves at L ~ 15 and fill the flux tube at all latitudes. At greater and smaller distances the 'solar wind' protons will experience little scattering by waves and tend to retain their anisotropy, except at Dione's L shell where the protons could also be effectively pitch angle scattered. Considering uncertainties in the observed power levels for the 'solar wind' protons and the fact that their scattering times scales will tend to be 14 times smaller than that for N^+ ions, they are more likely to be isotropized by these waves and precipitated into Saturn's upper atmosphere when compared to that for N^+ ions picked up in Titan's torus. Therefore, the waves will tend to enrich N^+ ions relative to protons. In contrast to the N^+ ions which are born with a large pressure anisotropy with $T_\perp/T_{||} >> 1$, the 'solar wind" protons could have a pitch angle distribution which was more isotropic at the time of injection and thus tend to fill a flux tube at all latitudes. Furthermore, if the injection energy of 'solar wind' protons is considerably greater than keV energies, then they will experience higher levels of pitch angle scattering, which will make them more isotropic in pitch angle, tend to fill flux tubes at all latitudes and experience significant precipitation within the inner magnetosphere for L < 10. N^+ ions injected at higher energies as previously discussed would not experience significant pitch angle scattering via waves and would be enriched relative to protons within the inner magnetosphere, while retaining their original pitch angle distribution which could also have $T_\perp/T_{||} >> 1$. Finally, we make note of the charge exchange lifetimes for protons and N^+ ions. Outside L ~ 15 charge exchange losses for N^+ ions are not important, while inside this distance charge exchange losses become comparable to transport time scales. In the case of protons charge exchange losses are important at all radial distances so that the 'solar wind' source of hot keV protons in the outer magnetosphere must be considerable larger than that for the Titan torus hot keV N^+ ions in order to dominate the energetic ion fluxes within Saturn's inner magnetosphere. Therefore, this mechanism will tend to enrich energetic N^+ ions relative to energetic protons within Saturn's inner magnetosphere (Here, we note the O^+ will also charge exchange efficiently).

We note that the above calculations only include power due to field aligned propagating Alfven waves, while compressional waves with k vectors perpendicular to $\vec{B}$ in the ϕ

direction have power levels nearly two orders of magnitude greater than the power in Alfvenic waves. But, it is not expected that these waves will be effective in scattering ions into the loss cone or making them isotropic. These waves with $k_{\perp} >> k_{ll}$ may be effective in violating the 3rd adiabatic invariant and contribute to the radial diffusion of the ions (Schultz and Lanzerotti, 1974).

At L ~ 15 there is substantial power in the waves so that the pitch angle diffusion time scale is only $\tau_{\alpha\alpha}$ ~ 1.74 hours for 384 keV protons in resonance with these waves. Here we note that these power levels are relatively high when compared to other periods analyzed by Lepping et al. (1986, 2004). A possible explanation for this is that the spacecraft is near the outer boundary of the plasma sheet where the plasma density drops abruptly outside L ~ 15 (see Sittler et al., 1983), and islands of plasma are becoming detached from the plasma sheet (Goertz, 1983, Curtis et al., 1986). This issue is also discussed in Lepping et al. (1986, 2004) for the outer magnetosphere in general. Therefore, we could be within a region of localized wave generation and turbulence as originally suggested by Goertz (1983). The LECP data also does not display detectable losses at L ~ 15 (Armstrong et al., 1983), especially in the case of 384 keV protons, so that radial transport time scales must be shorter than the strong diffusion limit $\tau_{sd,0}$ ~ 15 days. If we used the estimated transport time scale τ_R ~ 25 days based on our calculations in section 3.0, then this condition is violated and one would expect some precipitation losses. But, if one uses the transport time scale τ_R ~ 5 days estimated by Richardson et al. (1998) at Dione's L shell, then radial transport time scales could be shorter than $\tau_{sd,0}$ ~ 15 days and precipitation losses would be small for the energetic protons as observed. If, the transport times are τ_R ~ 25 days, and precipitation losses are small, then maybe the composition at these higher energies is dominated with heavy ions such as N^+ (i.e., resonance frequency outside main power spectrum peak). But, the energetic protons with E ~ 384 keV, if present, should be very isotropic.

Our satellite sweeping calculations for Rhea indicate that there will be a significant enrichment of N^+ relative to protons with transport time scales τ_R ~ 10 days, which is not inconsistent with our calculations of precipitation loses via wave scattering as discussed above. Using the Richardson et al. (1998) results, we estimated a lower limit for the predicted radial transport time scale τ_R ~ 2 days at L ~ 8.5. If so, then both precipitation and satellite sweeping by Rhea of the suprathermal ion population would be negligible at L ~ 8.5, but this is contrary to observations (see, Armstrong et al. (1983) and Paonessa and Cheng (1986a,b)). Richardson et al. (1998) did indicate that their model predictions would be more consistent with observations if radial transport declines with increasing distance between 7 and 12 R_S. One possibility for this they said was that the transport rate was dependent on the mass-loading rate. This is consistent with the OH and water group neutral clouds being confined within L ~ 7 (Richardson et al. (1998)) and the Titan neutral tori being confined outside L ~ 12 (Barbosa, 1987; Ip, 1992 and this work). This is also consistent with the Lepping et al. (1986, 2004) results as noted above. Therefore, the data when combining all observational constraints, are consistent with radial transport time scales $\tau_R \geq 10$ days at L ~ 8.5 with a tendency for N^+ ions to be enriched relative to protons. Finally, we note that the neutral hydrogen cloud, which has been reported from

Voyager UVS data (Shemansky and Hall, 1992) to extend throughout Saturn's magnetosphere, is not expected to be an important sorce of mass loading and the suprathermal populations discussed here, due to low mass. But, it could be an important charge exchange sink for suprathermal and energetic protons and heavy ions.

6.0 VOYAGER ION DATA AT DIONE'S L SHELL

In this section we examine the ion measurements in the vicinity of Dione's L shell, in the context of our proposed model where suprathermal N^+ ions originate within Titan's neutral torus and then diffuse radially inward to form Saturn's inner radiation belts. We will also explore various loss mechanisms for these nitrogen ions and the "solar wind" protons. This will provide further constraints on the radial diffusion coefficients.

6.1 Observations: In Figure 8 we show a three-component Maxwellian fit to the PLS ion data at the Voyager 1 outbound Dione L shell ring plane crossing. The PLS instrument includes four Faraday cup sensors (A-D) aligned in different directions. Within Saturn's magnetosphere the D cup is directed upstream towards the incoming corotating flow and is usually exposed to the highest ion fluxes, while A, B and C are pointing nearly perpendicular to this direction. Here, the suprathermal ion is assumed to be H^+, but the fit for this component, particularly in the D cup, is poor. In Figure 9 we show a fit to the same data, but now assuming N^+ for the suprathermal ion component. The fit is significantly better than that for H^+, especially in the D cup spectrum. In theory, we would expect a better fit assuming a water group ion for the suprathermal component, since within Saturn's inner magnetosphere one expects the neutral clouds to be dominated by water group molecules and atoms such as O^+, OH^+, H_2O^+ and H_3O^+ (see Sittler et al., 2004b). The density of the suprathermal component is $[O^+] \approx 3.9$ ions/cm^3, while the temperature of the O^+ suprathermal component is $T_{O+} \approx 2$ keV. The maximum pickup energy for H_2O^+ ions at Dione's L shell is $E_{MAX} \approx 1.4$ keV for a ring distribution, which is consistent with the observed temperature. In a qualitative sense, the fits for the suprathermal component would be improved if we used a shell distribution instead of a bi-Maxwellian. If so, these ions would be isotropic in pitch angle and tend to fill up a flux tube at all latitudes.

In Figure 10, we show a combined plot of PLS and LECP data during Voyager 1's outbound crossing of Dione's L shell, also near the ring plane crossing of this spacecraft. Water group ions are assumed for the PLS suprathermal ion component and LECP data above 10 keV was assumed to be dominated by N^+. The comparison across the energy gap looks good with a common power law between 1 keV and 3 MeV. Conserving the 1st and 2nd adiabatic invariants, using the mean energy of the PLS suprathermal N^+ component at Titan's torus and mapping to Dione's L shell, we obtain a mean N^+ energy greater than 100 keV. This would suggest that most of the LECP fluxes are N^+. Here, we note that for energies greater than 500 keV, the composition is thought to be dominated by protons (Paranicas et al., 2004). We have also super-imposed the electron intensities from Maurice et al. (1996). These electrons will be important for the radiolytic reactions taking place for depths greater than 1 micron in the surface ice of Dione. When the PLS suprathermal water group ions at Dione diffuse radially outward to Titan's torus they

may adiabatically cool to energies ~ 60-100 eV as observed for the cold component within the outer magnetosphere.

Pressure integrals over the Dione PLS spectra depend strongly on whether the ion is H^+ or O^+, the latter giving 2.6 nPa as compared to 0.1 nPa for H^+ at plasma energies and 1.1 nPa for the LECP ions inferred to be N^+. For O^+ this result differs from integrals for the Titan N^+ spectra giving comparable 0.1 nPa pressures at both PLS and LECP energies. In contrast, Maurice et al. (1996) found comparable pressures for plasma and energetic components of the electron population in Saturn's middle magnetosphere. The electron pressure is ~ 0.2 nPa. For magnetic pressure $B^2/8\pi \sim 2.5$ nPa at Dione's orbit the plasma β parameter, the ratio of plasma and magnetic pressure, is ~ 1 for an O^+ plasma component, 0.44 for energetic N^+, 0.08 for electrons and ~ 1.5 overall. Due to low magnetic field at Titan's orbit the $\beta \sim 10$ values are much higher, but even at Dione high β effects such as diamagnetism may be present.

6.2 Ion Losses and Transport Time Scales: In Table 2 we summarize the particle and field parameters that characterize the environment surrounding Dione, while Table 3 summarizes the parameters concerned with ion precipitation losses due to ion cyclotron waves known to be present around Dione's L shell. It also lists ion losses due to charge exchange and elastic-inelastic collisions with thermal ions and neutrals and subsequent suprathermal ion precipitation. Coulomb collision time scales for the thermal plasma are also given.

Table 2

Parameter	Value
L	6.3
N_e (#/cm^3)	35.0
T_e (eV)	10.0
[H^+] (#/cm^3)	2.1
[O^+] (#/cm^3)	29.0
[OH^+] (#/cm^3)	4.45
[H_2O^+] (#/cm^3)	3.6
T_{H+} (eV)	51
T_{O+} (eV)	261
T_{OH+} (eV)	278
T_{H2O+} (eV)	294
[O^+]* (#/cm^3)	3.9
T_{O+}* (eV)	2000.0
[H] (#/cm^3)	80.0
[O] (#/cm^3)	180.0
[OH] (#/cm^3)	250.0
[H_2O] (#/cm^3)	30.0
V_R (km/s)	53.0
B (nT)	80.0

* indicates suprathermal component

Table 3

Parameter	Protons	Heavy Ions (O^+)
E_{MAX} (MeV/G)	0.074	1.18
E_M (MeV/G)	0.796	0.796
F_{gyro} (mHz)	1200	76.0
α_L (Deg.)	2.55	2.55
F_{peak} (mHz)	50.0	50.0
E_R (MeV/G)	458.0	1.84
τ_B (sec)	244.0	1.54×10^4
$1/\tau_{sd,0}$ (sec^{-1})	2.1×10^{-5}	3.7×10^{-7}
δB (nT)	0.7	0.7
$P\Delta f_{MHD}$ (nT^2)	0.49	0.49
$D_{\alpha\alpha}$ (sec^{-1})	5.9×10^{-5}	3.7×10^{-6}
τ_{iso} (years)[1]	116	16
$\tau_{protons}$ (years)[1]	3	NA
τ_{heavy} (years)[1]	NA	116
τ_{i-e} (years)[1]	3	3
$\tau_{elastic+inelastic}$ (years)[2]	3.2	3.1

1. Coulomb Collisions
2. Estimated using range data in Figure 6

At thermal energies, in the vicinity of Dione, Richardson et al. (1998) estimated charge exchange lifetimes for H^+ to be $\tau_{cx} \sim 10^5$ s, $\tau_{cx} \sim 10^5$ s for O^+, $\tau_{cx} \sim 2 \times 10^6$ s for H_2O^+ and plasma transport time scale $\tau_R \sim 5$ days. With regard to Coulomb collisions for the thermal population all time scales are much longer than the time scales due to diffusive transport, charge exchange losses, and pitch angle scattering of the suprathermal ions by ion cyclotron waves. From Richardson et al. (1998) the isotropization time scales for thermal O^+ are $\tau_{iso} \sim 16$ years, $\tau_{iso} \sim 116$ days for thermal H^+ and $\tau_{iso} \sim$ 3-4 minutes for thermal electrons. Energy transfer time scales for O^+ to H^+ is $\tau_{protons} \sim 3$ years, $\tau_{heavy} \sim$ 116 days for H^+ to O^+ and $\tau_{i-e} \sim 1.5$ years for ions to electrons. Therefore, except for the isotropization of thermal electrons, the Coulomb collision time scales for isotropization and energy transfer between species are much longer than times for diffusive transport, pitch angle scattering by waves and precipitation induced by waves. In the case of suprathermal ions the Coulomb collision time scales will be even longer than that for the thermal ions because of the speed dependence of the Coulomb cross-section.

The charge exchange cross-sections for suprathermal N^+ ions with energy E ~ 100 keV are as follows: $\sigma_{N\text{-}H} \sim 4.6 \times 10^{-16}$ cm^2 (Phaneuf et al., 1978), $\sigma_{N\text{-}O} \sim 6.0 \times 10^{-16}$ cm^2 (Lo et al., 1971), $\sigma_{N\text{-}OH} \sim 6.0 \times 10^{-16}$ cm^2, and $\sigma_{N\text{-}H2O} \sim 6.0 \times 10^{-16}$ cm^2 (Note, assumed cross-sections for OH and H_2O the same as O) and the correspondingly estimated N^+ lifetime is $\tau_{cx} \sim 10^5$ s or 1.35 days. For these same ions the estimated resonance frequency is around 4 mHz, which lies below the main peak in the power spectrum, so the $D_{\alpha\alpha} \sim 3.7 \times 10^{-8}$ sec^{-}

[1] or $\tau_{\alpha\alpha} \sim 313$ days and if the transport time scales is $\tau_R \sim 5$ days then precipitation losses will be negligible. The strong diffusion limit for these ions will be only $\tau_{sd,0} \sim 3.4$ days, so we have weak pitch angle scattering. If we use $\tau_R \sim 5.25$ days at L ~ 20 and assume $D = D_0L^3$ then at Dione's L shell the transport time scale $\tau_R \sim 168$ days. Even if precipitation losses were important under these conditions, charge exchange losses will still dominate.

If we consider "solar wind" protons with the same energy E ~ 100 keV, as we have used for N^+, then the appropriate charge exchange cross-sections will be as follows: $\sigma_{H\text{-}H} \sim 1.24\text{x}10^{-17}$ cm^2 (McClure, 1966), $\sigma_{H\text{-}O} \sim 1.06\text{x}10^{-16}$ cm^2 (Thompson et al., 1996), $\sigma_{H\text{-}OH} \sim 9.4\text{x}10^{-16}$ cm^2 (i.e., assumed to be the same as H_2O), and $\sigma_{H\text{-}H2O} \sim 9.4\text{x}10^{-16}$ cm^2 (Gobet et al., 2001). Using these numbers, we estimate the charged exchange lifetime for protons to be $\tau_{cx} \sim 1$ day. So, the charge exchange lifetime for both protons and N^+ 100 keV ions are about the same and neither is enriched relative to each other due to charged exchange losses. For these protons the estimated resonance frequency is 96 mHz, which is above the main peak in the wave power spectrum. Under these conditions $D_{\alpha\alpha} \sim 2.9\text{x}10^{-6}$ sec^{-1} or $\tau_{\alpha\alpha} \sim 3.9$ days ~ $\tau_R \sim 5.25$ days > $\tau_{cx} \sim 1$ day. So, in summary, charge exchange losses dominate all other mechanisms in the vicinity of Dione's L shell for both E ~ 100 keV protons and N^+ ions, and are short compared to the relatively fast transport time scales τ_R ~ 5 days estimated by Richardson et al. (1998).

We will now estimate the various loss mechanisms for protons (i.e., E ~ 366 keV) and N^+ (i.e., E ~ 1.47 keV) that are in resonance with the main peak in the magnetic field power spectrum as reported by Smith and Tsurutani (1983). The relevant numbers can be found in Tables 2 and 3 for pitch angle scattering time scales. The pitch angle scattering diffusion coefficient for the pickup water group ions with energy $E_O \sim 1.3$ keV is then estimated to be $D_{\alpha\alpha} \sim 4.3 \times 10^{-6}$ sec^{-1} or scattering time scale $\tau_{\alpha\alpha} \sim 2.7$ days. Assuming a minimum resident time scale of $\tau_R \sim 5$ days, the pickup water group ions will be effectively scattered from ring distributions to either a shell distribution or a Maxwellian distribution (i.e., isotropic in pitch angle). The PLS data do suggest a shell distribution, but a more quantitative analysis would be required to confirm this. In the strong diffusion limit for the $E_O = 1.3$ keV ions the minimum precipitation time scale is $\tau_{sd,0}(O^+) \sim 29$ days so we are at the strong diffusion limit. But, if $\tau_{sd,0}(O^+) >> \tau_R \sim 5$ days, then precipitation losses will be small, so that the main function of the waves will be to make the ions isotropic in pitch angle..

The energetic protons $E_R(p) \sim 366$ keV in resonance with the ion cyclotron waves are estimated to have a pitch angle diffusion coefficient $D_{\alpha\alpha} \sim 6.9 \times 10^{-5}$ sec^{-1} or wave scattering time scale $\tau_{\alpha\alpha} \sim 4$ hours. The strong diffusion time scale for these protons is $\tau_{sd,0} \sim 13.5$ hours, so we are at the strong diffusion limit and precipitation losses are expected to be important since $\tau_R \sim 5$ days >> $\tau_{sd,0}$. Charge exchange lifetimes for these protons are estimated to be $\tau_{ex}(H^+) \sim 12$ days and thus not an important loss mechanism when compared to wave scattering. In the case of energetic nitrogen ions, $E_{N+} \sim 366$ keV, their estimated pitch angle diffusion coefficient is $D_{\alpha\alpha} \sim 2.1\text{x}10^{-7}$ sec^{-1} or corresponding scattering time scale of $\tau_{\alpha\alpha} \sim 55$ days. So, here precipitation losses are negligible and

wave scattering will tend to enrich N^+ relative to protons at these high energies, but this is negated by the relatively short charge exchange lifetimes of $\tau_{ex} \sim 1$ day of N^+ ions.

In summary, the lifetime of both energetic protons and N^+ ions are ~ 1 day, which is short compared to radial diffusion time scales as estimated by Richardson et al. (1998). Therefore, if energetic N^+ ions cannot penetrate inside of Dione's L shell because of charge exchange losses, then the same should be true for energetic protons.

7.0 ION DEPOSITION RATES AND RADIOLYSIS AS A FUNCTION OF DEPTH FOR DIONE'S SURFACE

In this section we will estimate the ion implantation rates and radiolysis as a function of depth for the icy surface of Dione using the intensities shown in Figure 10 and the published electron intensities by Maurice et al. (1996) which covers the energy range from 10 eV to 2 MeV. Below 10 keV we used the composition shown in Figure 9 for PLS where the suprathermal component is assumed to be O^+, while at energies greater than 10 keV we assumed a composition of N^+. Delitsky and Lane (2002) assumed the nitrogen was 10% of the thermal plasma. Here, we propose that most of the nitrogen is at energies greater than 10 keV and will be deposited deeper into the ice. As reported in Richardson et al. (1998), the source of water molecules within Saturn's inner magnetosphere is $S_W \sim 1.4 \times 10^{27}$ mol/s, while the source of hot nitrogen atoms within Saturn's outer magnetosphere is $S_{N*} \sim 4.5 \times 10^{25}$ atoms/s. This number does not include the source of thermal nitrogen ions $S_{N+} \sim 4 \times 10^{24}$ ions/sec into Saturn's outer magnetosphere due to scavenging of Titan's atmosphere and ionosphere by the magnetospheric plasma (see Hartle et al. 1982; Eviatar and Podolak, 1983). In both cases a majority of the hot ions from the neutral torus and corresponding thermal ions from scavenging will be transported outward and lost to the magnetopause. Therefore, the Delitsky and Lane (2002) estimate is at least an order of magnitude too high and that a rough minimum energy for N^+ ions is ~ 10 keV. Even though our neutral cloud calculations in Figure 1 show significant nitrogen densities within Saturn's inner magnetosphere, this model calculation did not include the shorter ionization and charge exchange time scales $\tau_{loss} < 10^6$ s within the inner magnetosphere due to its higher plasma densities. The calculations by Smith et al. (2004) do show significant production rates of nitrogen pickup ions as close in as Dione where they do consider the presence of the plasma sheet and corresponding enhanced ionization rates. These results do indicate that there could be an important source of low energy nitrogen ions within Saturn's inner magnetosphere. For our ion implantation and radiolysis calculations we will use the codes developed by Cooper et al. (2001) for the icy Galilean satellites.

In Figure 11 we show the ion implantation rate in terms of ion density per year as a function of surface depth. It is useful to know for the following discussions that the column density of water molecules in ice for a depth of 1 cm is ~ 3×10^{22} mol/cm^2. We will use 10% of this as an upper estimate for our accumulated implanted column densities for N^+ within the ice and corresponding accumulation time scale τ_{acc}. Figure 11 shows that within a few mono-layers of the surface the dominant implanted ions are O^+ and H^+ and the corresponding accumulation time scales $\tau_{acc} \sim 1.2$ Myrs for O^+ and $\tau_{acc} \sim 3$ Myrs

for H^+. The N^+, will penetrate below 1 micron, with an effective accumulation time τ_{acc} ~ 30 Myrs. The time scale for meteoritic gardening over a depth of 1 cm is about 10^4 years (Cooper et al., 2001), which is far shorter than our implantation time scales. Therefore, it is reasonable to assume that the implanted nitrogen will be uniformly distributed over such a depth. For longer time scales the meteoritic gardening will extend down to ~ 1 meter depth. Cooper et al. (2001) also argue that these ions will be buried faster by impact ejecta than they can removed by sputtering or sublimation. Actual regolith depth depends on geologic age of the surface, which in the case for Dione is > 1 Gyrs (Morrison et al. (1984)). This argument should be even more applicable at Saturn where the icy satellites are colder and the sputtering rates are considerably less than that at the Galilean satellites, except for may be Callisto. The gravitational focusing factor, used for the above calculations, $f_G \sim 1 + (v_{esc}/v_\infty)^2 < 1.7$ at Saturn. This estimate is comparable to but less than that for Jupiter with $f_G < 2.8$ for Europa, Ganymede and Callisto (Cooper et al., 2001). At Saturn we use $v_{esc} \sim 12$ km/s (i.e., at Rhea's orbital position) and $v_\infty \sim 14$ km/s. Therefore, meteoritic impact rates at Saturn are comparable to but less than that at Jupiter, but more than offset by the higher sputtering and sublimation rates for the Galilean icy satellites.

Delitsky and Lane (2002) suggest a chemistry model that might occur due to nitrogen implanted into the water ice. The nitrogen was first converted into nitric oxide, NO, and then into other nitrogen molecules. In Figure 12, similar to that done for Figure 11, we show the dosage time for radiological processes to occur for Dione, using the ion and electron intensities shown in Figure 10. For depths greater than 1 mm, the radiolysis is dominated by the energy deposited by penetrating energetic electrons (see Johnson et al., 2004). At depths, ~ 1 micron, the energetic nitrogen ions dominate the radiolysis, while within a few mono-layers of the surface O^+ and H^+ dominate the radiolysis. Near the surface the dosage time scale at 0.1 microns is about 50 years, while at Europa it is about 3.5 years and Callisto about 150 years. At 1 micron the radiolysis time scale, is about t ~ 500 years. By using the intensities shown in Figure 10, the nature and depth distribution of the energy deposition is different from that used by Delitsky and Lane (2002). But, most importantly, our estimated net energy fluxes are greater by an order of magnitude than those in Delitsky and Lane (2002). In the case of ion energy flux they estimated an energy flux ~ 1.7×10^8 keV/cm^2-s, while we estimate an energy flux ~ 6.5×10^7 keV/cm^2-s for the thermal plasma and ~ 5.5×10^7 keV/cm^2-s for the E > 10 keV hot plasma, for a total ion energy flux ~ 1.3×10^8 keV/cm^2-s. In the case of electrons we estimate an energy flux for PLS electrons ~ 2.6×10^8 keV/cm^2-s and for the LECP-CRS electrons we estimate ~ 1.5×10^9 keV/cm^2-s, for a total electron energy flux ~ 1.8×10^9 keV/cm^2-s. In the case of Delitsky and Lane (2002), they estimated an electron energy flux ~ 2.2×10^8 keV/cm^2-s, which is an order of magnitude lower than our estimate. To compute our energy flux, EF, we used the expression

$$EF = \pi \int j(E) E dE$$

for which E is the particles relativistically correct total kinetic energy (see Cooper et al., 2001). This integral has a stronger weighting at higher energies than that used by Delitsky and Lane (2002). As expected, their numbers are closer to what we call the

contribution from PLS, where most of the electron density resides. The electron energy spectrum is highly non-Maxwellian, and accounts for the large discrepancy.

For an individual species, Delisky and Lane (2002) estimated the column densities for a wide range of molecules using the formula N = EGt, for which, E is the energy flux (keV/cm^2-s), G is the radiolysis yield or "G value" in units of molecules/100 eV of energy deposited, and t is the time. This is applicable only if the percentages are very small. They used t =1000 years, which is subjective, but comparable to the meteoritic gardening time scale at a depth of 1 mm (see Cooper et al., 2001), which is essentially the optical depth for composition measurements if grain sizes for optical scattering are something like 100 microns. Because our energy flux is an order of magnitude greater than theirs, we need use a time t ~ 100 years in order to get molecular abundances similar to that computed by Delitsky and Lane (2002). We have converted their numbers to a percentage of the column density for ice $N_W \sim 3.3 \times 10^{22}$ mol/cm^2. This was done as a means of estimating what fraction of the water molecules sputtered into Dione's atmosphere is composed of these molecules, and whether the Cassini Plasma Spectrometer (CAPS) Ion Mass Spectrometer (IMS) will be able to detect them as pickup ions (see Sittler et al., 2004a). If we sum up all the molecules relative to the water molecules in the ice we get 21.7% of all the water molecules are composed of the various molecules listed in Delitsky and Lane (2002). This large percentage violates the original assumption made when using these G factors and underscores the fact that one cannot decouple the reaction between the various species derived by Delitsky and Lane (2002).

Sputtering could be an important loss mechanism for the icy surface of Dione and removal of implanted ions and resulting chemistry in the ice. For example, the sputtering rate is $S_D \sim 10^{26}$ mol/s (Jurac et al., 2001a,b), Dione's surface area is $A_D = 4\pi R_D^2 \approx 4\times10^{16}$ cm^2, $R_D = 560$ km, so that flux of water molecules leaving Dione's surface is $F_D = S_D/A_D \sim 2.53 \times 10^9$ mol/cm^2/s and the time scale to remove 1 cm of ice from Dione's surface is $\tau_{sput} = N_W/F_D \sim 4 \times 10^5$ years $<< \tau_{acc}(N^+) \sim 30 \times 10^6$ years). But, the rate of meteoritic gardening down to a 1 cm depth is $\sim 10^4$ years, which is $<< \tau_{sput}$. So, the various nitrogen and hydrocarbon molecules could be buried deeper in the ice and survive losses due to sputtering. We should also note that the sputtering rates are higher for those molecules that are more volatile or outgas at higher rates for formation of an exosphere or corona around Dione (see Sittler et al., 2004a). For example, one can estimate the source rate for molecules into this atmosphere as follows: $S_{atm} \sim (dN/dt)A_D \sim (3.3 \times 10^{20}$ mol/cm$^2)(4\times10^{16}$ cm$^2)/(1000$ years$) \sim 4.2\times10^{26}$ mol/s. We then need to estimate scavenging time scale for removing the atmospheric molecules. This is related to the charge exchange lifetime $\tau_{cx} \sim 2\times10^6$ s, ionization time scale $\tau_{ion} \sim 5 \times 10^6$ s and the elastic scattering time scale $\tau_{elastic} \sim 1.8\times10^6$ s (i.e., used collision cross-section $\sigma \sim 3\times10^{-15}$ cm^2 from Eviatar and Podolak (1983) and Book (1977)), which gives us an overall scavenging time scale of $\tau_{scav} \sim 8\times10^5$ s. The estimated scale height of this atmosphere is h ~ 120 km. Combining these we can estimate the atmospheric density $n = (4.2\times10^{26})(8 \times 10^5)/(5.8\times10^{23}$ cm$^3) \sim 5.8\times10^8$ mol/cm^3. Evidently, if true, this atmosphere was not detected by Voyager. This estimate is lower by several orders of magnitude than that given by Sittler et al. (2004a), who based their estimate, $n \sim 8\times10^{11}$ mol/cm^3, on an observed column density of $\sim 2 \times 10^{16}$ mol/cm^2 for ozone at Dione and corresponding

inferred column density of 10^{19} mol/cm^2 for O_2 (Noll et al., 1997). The estimate by Sittler et al. (2004a) was more empirically based and only represented an upper estimate. If such an atmosphere is present, the actual atmospheric density probably resides between these two limits and its detection by Cassini should be a high priority. In order for CAPS to detect these species their number should be at the 1% level or greater relative to the number of water molecules in the ice. Also, CAPS should be able to detect an atmosphere or corona as estimated here and in Sittler et al. (2004a). Our calculations do indicate that species such as N, NO, NO_2, HNO_3, N_2, and N_2O if at the 1-10% level relative to water ice, should be detectable by CAPS.

Delitsky and Lane (2002) did not assume the presence of ammonia in the ice from the primordial formation of the Saturn System. The presence of ammonia within Titan's crust is thought to be significant because of its dense N_2 atmosphere (e.g., Sittler et al., 2004a) and it has been proposed that the activity suggested by Encleadus's young surface is due to ammonia (e.g., Stevenson 1982). . We also note, that the dominant ion within Titan's ionosphere may not be N_2^+, but rather H_2CN^+ (Hartle et al., 1982; Keller et al., 1998), $C_2H_5^+$ (Keller et al. 1992) and CH_5^+ can dominate at higher altitudes (Keller et al., 1998). Therefore, significant amounts of C^+ could find itself within the inner magnetosphere as we have suggested for N^+. Delitsky and Lane (2002) assumed that CO_2 was already present in the ice. Here we note that C^+ could be implanted into the ice.

8.0 LABORATORY EXPERIMENTS PERFORMING ION IRRADIATION-RADIOLYSIS OF ICY SURFACES AND MEASURING IR ABSORBANCE SPECTRA FOR SURFACE COMPOSITION MEASUREMENTS.

Saturn's icy satellites, when implanted with nitrogen are expected to produce new molecules in an ice matrix or as inclusions in ice. We now consider some laboratory data using irradiation techniques developed by Moore and Hudson (2000) to confirm the possible presence of the nitrogen species discussed above. At present, only MeV protons are used in laboratory ice irradiations and IR spectroscopy is used to follow the corresponding chemistry that results. In terms of estimating the effect of radiolysis and corresponding chemistry for the same dose the energetic protons produce to first order the same effect as the energetic nitrogen ions. The implantation of N^+ and O^+ in the ice can be simulated by mixing N_2 and O_2 in the ice and then irradiating this ice mixture with energetic protons. To determine likely products, we examined an ice mixture of $H_2O + N_2 + O_2$ (3:1:1). When such a laboratory ice is condensed at 20 K and warmed to 100 K (a temperature more relevant to the icy surfaces at Saturn), most of the N_2 and O_2 sublime. If irradiations are performed at 100 K there is not enough N_2 and O_2 trapped in the ice to make IR-detectable products. Therefore, we irradiated the ice mixture at 20 K. Figure 13 shows the products observed, NO, NO_2, N_2O, O_3 and H_2O_2, which have lower vapor pressures than N_2 and O_2. When the irradiated sample was warmed to 100 K, N_2O, O_3 and H_2O_2 were still observed. Therefore, several of the species discussed by Delitsky and Lane (2002) were observed in this simulation. Most of the G factors used by Delisky and Lane (2002) were inferred from related experimental data, so there is considerable uncertainty. The results shown in Figure 13, shows some of the molecules produced in the ice, such as NO and NO_2, could sublimate from the ice and contribute to an exosphere

or corona around Dione (see previous section). Meteoritic gardening will tend to mix these molecules to depths deeper than 1 cm so that they may remain trapped in the ice at the higher temperatures of 100 K. If so, they may still be detectable by CAPS via sputtering of these molecules from the icy surface and their subsequent ionization in the vicinity of Dione (see Sittler et al., 2004a).

It is important to note the measurements by Strazzulla et al. (2003), where they irradiated icy surfaces at temperatures between 16 K and 77 K with either 30 keV C^+ or N^+ ions. In the case of C^+ they did detect CO_2 and CO in the ice after irradiation. But for 30 keV N^+ ions incident on the ice, they only found nitrogen molecules if they had NH_3/CH_4 already in the ice. If the penetration depths and sputtering rates are such that the implanted N is removed efficiently or if a more volatile species such as N2 formed and removed, the proposed chemistry, based on initially forming NO, might not occur. Therefore, the nitrogen species due to implantation might be difficult to observe spectroscopically. However, in steady-state nitrogen species must be ejected into the gas-phase at a rate equivalent to the implantation rate. Therefore, such species will be observable by Cassini in the plasma.

9.0 SUMMARY AND CONCLUSIONS

In this paper we have made the case that Titan is the source of a large atomic nitrogen torus surrounding Saturn within the outer magnetosphere with L ~ 20 (Eviatar and Podolak, 1983; Eviatar et al., 1983; Barbosa, 1986; Ip, 1992) and that this cloud will be the source of keV pickup nitrogen ions (see Lazarus and McNutt, 1983). A subset of these keV nitrogen ions will then be transported into Saturn's inner magnetosphere where they will be energized by conserving the first and second adiabatic invariants. We suggest they may dominate the energetic ion population (i.e., enrichment process). These energetic nitrogen ions will then bombard the icy surfaces of the moons within the inner magnetosphere and create the complex nitrogen chemistry in impact regolith layers on their icy surfaces, which may otherwise have low nitrogen abundances due to dominance of water group ions in the plasma at Dione.

We reviewed the estimates of the source strength of hot neutral atoms from Titan. The primary uncertainty for estimating the source strength is the height of the ionopause and the access of magnetospheric plasma to the exobase or lower altitudes (Ip, 1992). Assuming an energy distribution with $f(E) = 1/(E+U)^2$ and U = 0.3 eV or a mono-energetic spectrum with ejection speeds ~ 1 km/s, we presented results of a Monte Carlo model of the nitrogen torus with uniform life time against ionization of $\tau_{N0} \sim 3 \times 10^7$ s. This model showed a neutral torus centered on Titan's orbit and extending into the inner magnetosphere with a thickness of ± 2 R_S near Titan. Using this source rate and the Voyager PLS observations, we estimated resident or transport time scales for the pickup ions to be ~ 5.25 days. This is greater than the lower limit estimated from radial diffusion coefficients as determined by Paonessa and Cheng (1986). The PLS data also indicates that within this torus the suprathermal ion component is confined to the equatorial plane so that $T_\perp / T_{ll} >> 1$. This is consistent with our calculations that give a torus thickness < 4 R_S.

We also looked into the importance of a solar wind source. This could also provide keV protons and alpha particles within Saturn's outer magnetosphere and be the source of energetic protons within Saturn's inner magnetosphere. We determined that "solar wind" protons could be competitive relative to suprathermal N^+ ions from the Titan torus, but, parameter uncertainties are too high to make a definitive statement. However, the PLS suprathermal ion measurements give a better fit if we assume N^+ than if we assume protons (i.e., Mach number effect). The energy spectrum with both PLS and LECP data combined gives a better match with nitrogen ions dominating the LECP fluxes and the PLS suprathermal fluxes. But, the paper by Maclennan et al. (1982) would favor a proton composition within Saturn's outer magnetosphere. Finally, the re-analysis of the Voyager 1 plasma data by Sittler et al. (2004b) showed that the keV component observed by PLS was in fact a heavy ion component like N^+ because of finite gyro-radius effects.

Consistent with this, we looked into the enrichment of N^+ ions relative to protons as they diffuse radially inward. We compared both satellite sweeping, precipitation losses in the vicinity of Rhea's L shell and charge exchange losses. We found all losses to be comparable to transport time scales ~ 10 days. We showed that all three mechanisms will tend to deplete protons relative to N^+ ions within Saturn's inner magnetosphere. Furthermore, the MHD waves reported by Lepping et al. (1986, 2004) for $8.5 < L < 16.9$ will tend to scatter the protons and make them isotropic, while transport time scales may be short enough so that $T_\perp / T_{ll} >> 1$ for the nitrogen ions as they are transported into the inner magnetosphere. In both cases for protons and N^+ ions precipitation losses are at the weak pitch angle limit in the vicinity of Rhea. If the protons are isotropic they will tend to fill the flux tubes completely and be observable at high latitudes. In the case of N^+, with $T_\perp / T_{ll} >> 1$, the nitrogen ions will be confined near the equatorial plane and not be observable at high latitudes. At Dione, where enhanced levels of ion cyclotron waves are observed (Smith and Tsurutani, 1983; Barbosa, 1993), pitch angle scattering will be at the strong limit for energetic protons with energies ~ 400 keV and low energy suprathermal oxygen ions with $E_{O+} \sim 1.4$ keV. In the case of energetic protons precipitational losses will be important and competitive with charge exchange losses, while for keV O^+ the time scale for the strong diffusion limit $\tau_{sd,0} >> \tau_R \sim 5$ days the transport time scale as required by Richardson et al. (1998). Therefore, these pickup ions will be isotropized by the waves, but precipitational losses will be small. If so, in contrast to the pickup ions within the Titan nitrogen torus, these suprathermal water group ions are expected to be more isotropic in pitch angle, tend to form shell distributions and fill flux tubes at all magnetic latitudes. It must be said that the radial diffusion coefficient has the appearance of being highly uncertain; if we use our estimate at L ~ 20 ($\tau_R \sim 5.25$ days), we get $\tau_R \sim$ 68 days at L ~ 8.5, while at L ~ 6.3 ($\tau_R \sim 5$ days) we get $\tau_R \sim 2$ days at L ~ 8.5. So, under these circumstances the radial diffusion coefficient has an uncertainty by more than an order of magnitude. But, when we consider the scattering time scales, L shell sweeping, observed particle losses reported by Armstrong et al. (1983) and the fact that Richardson et al. (1998) suggested that transport time scales could be longer between L ~ 7-12, transport time scales $\tau_R \sim 10$ days seems highly probable at L ~ 8.5.

Here, we note that Eviatar et al. (1983) proposed that O^+ ions could charge exchange with the A-ring's hydrogen atmosphere just outside it's outer edge and produce a source of oxygen atoms within Saturn's outer magnetosphere (i.e., gravitationally bound to Saturn) with a source strength $S_O \sim 1.4x10^{26}$ atoms/s. It was also noted that the charge exchange process inside of 4 R_S can occur by ion-molecule orbiting interactions which would recycle oxygen and other water products throughout the magnetosphere. An oxygen torus that extends to the outer magnetosphere can produce a hot keV O^+ component similar to the hot keV N^+ ions that diffuse radially inward and contribute to Saturn's energetic ion component within Saturn's inner magnetosphere. Composition measurements within the equatorial plane of Saturn's magnetosphere by the CAPS (Young et al., 2004) and MIMI (Krimigis et al., 2004) instruments will determine which mechanism is dominant.

We then combined the PLS and LECP data during the Voyager 1 ring plane crossing of Dione's L shell. The data is consistent with thermal protons and water group ions. The PLS suprathermal ion fluxes were best fit as being water group ions which we identified as being O^+ ions. But, for the LECP data we assumed the dominant ion was N^+ instead of O^+. Using algorithms developed by Cooper et al. (2001) for the Galilean satellites, we computed the implantation rates and dosage rates for radiolysis as a function of depth for H^+, O^+ and N^+. In the case of nitrogen they were considerably more energetic than the thermal nitrogen plasma used by Delitsky and Lane (2002). Using their highly uncertain G-values the nitrogen products would be a considerable fraction of the ejected water products, which is not likely. However, many of the species proposed have been observed in our laboratory as trapped molecules in an ice matrix: were N, NO, NO_2, HNO_3, N_2, and N_2O. These may be observable by the CAPS instrument during a targeted flyby of Dione from the sputtering of Dione's icy surface and their corresponding ionization and formation of ring distributions (see Sittler et al., 2004a). CAPS detection of the freshly formed ions maybe more sensitive than IR absorbance spectra or that an exosphere surrounding Dione composed of the more volatile species would be observable by both VIMS NIR remote sensing measurements and CAPS *in situ* measurements of pickup ions during targeted flybys of Dione.

The results presented here provide numerous predictions for the Cassini Mission during the tour phase with regard to the distribution of nitrogen atoms and ions within Saturn's magnetosphere in both coordinate and velocity space. We have also made predictions with regard to energy and pitch angle distributions for both protons and nitrogen ions, the implantation of H^+, O^+ and N^+ ions within the surface ice of Dione, and the corresponding nitrogen chemistry within the ice of Dione driven by ion and electron bombardment upon its surface.

10.0 ACKNOWLEDGEMENTS

Some of the work presented in this paper was performed at the Jet Propulsion Laboratory, California Institute of Technology under contract with NASA. At Goddard Space Flight Center, ECS, we acknowledge support from the CAPS Cassini Project. The work of REJ and HTS at Virginia was supported by the CAPS Cassini Instrument and by NASA's Planetary Atmosphere's Program. JFC also acknowledges support through Raytheon

from NASA's Planetary Atmospheres Program and the Space Science Data Operations Office at NASA Goddard Space Flight Center.

REFERENCES

1. Armstrong, T.P., M.T. Paonessa, E.V. Bell II and S.M. Krimigis, Voyager observations of Saturnian ion and electron phase space densities, *J. Geophys. Res.*, **88**, 8893, 1983.
2. Barbosa, D.D., Medium energy electrons and heavy ions in Jupiter's magnetosphere: Effects of lower hybrid wave-particle interactions, *J. Geophys. Res.,* **91**, 5605-5615, 1986.
3. Barbosa, D.D. and A. Eviatar, Planetary fast neutral emission and effects on the solar wind: A cometary exosphere analog, *Astrophys. J.,* **310**, 927-936, 1986.
4. Barbosa, D.D., Titan's atomic nitrogen torus: Inferred properties and consequences for the Saturnian aurora, *Icarus,* **72**, 53, 1987.
5. Barbosa, D.D., Theory and observations of electromagnetic ion cyclotron waves in Saturn's inner magnetosphere, *J. Geophys. Res.*, **98**, 9345, 1993.
6. Baum, W.A., T. Kreidl, J.A. Westphal, G.E. Danielson, P.K. Seidelmann, D. Pascu and D.G. Currie, Saturn's E Ring, *Icarus*, **47**, 84, 1981.
7. Book, D. L., Revised and enlarged collection of plasma physics formulas and data, *NRL Memo. Rep.*, **3332**, Naval Res. Lab., Washington D. C., 1977.
8. Brecht, S. H., J. G. Luhmann and D. J. Larson, Simulation of the Saturnian magnetospheric interaction with Titan, *J. Geophys. Res.*, **105**, 13,119-13,130, 2000.
9. Bridge, H.S., J.W. Belcher, R.J. Butler, A.J. Lazarus, A.M. Mavretic, J.D. Sullivan, G.L. Siscoe and V.M. Vasyliunas, The plasma experiemtn on the 1977 Voyager Mission, *Space Sci. Rev.,* **21**, 259, 1977.
10. Broadfoot, A. L., B.R. Sandel, D.E. Shemansky, J.B. Holberg, G.R. Smith, D.F. Strobel, J.C. McConnell, S. Kumar, D.M. Hunten, S.K. Atreya, T.M. Donahue, H.W. Moos, J.L. Bertaux, J.E. Blamont and R.B. Pomphrey, Extreme ultraviolet observations from Voyager 1 encounter with Saturn, *Science,* **212**, 206-211, 1981.
11. Carbary, J. F., S. M. Krimigis, and and W.-H. Ip, Energetic particle measurements of Saturn's satellites, *J. Geophys. Res*., **88(A11)**, 8947-8958, 1983.
12. Carlson, R. W., A tenuous carbon dioxide atmosphere on Jupiter's moon Callisto, *Science*, **283**, 820-821, 1999.
13. Connerney, J.E.P., M.H. Acuna and N.F. Ness, Currents in Saturn's magnetosphere, *J. Geophys. Res.,* **88**, 8779, 1983.
14. Cooper, J. F., Nuclear cascades in Saturn's rings:Cosmic ray albedo neutron decay and origins of trapped protons in the inner magnetosphere, *J. Geophys. Res.*, **88**, 3945-3954, 1983.
15. Cooper, J. F., E. C. Sittler, Jr., S. Maurice, B. Mauk, and R. S. Selesnick, Local time asymmetry of drift shells for energetic electrons in the middle magnetosphere of Saturn, *Adv. Sp. Res*., **21(11)**, 1479-1482, 1998.

16. Cooper, J. F., R. E. Johnson, B. H. Mauk, H. B. Garrett and N. Gehrels, Energetic ion and electron irradiation of the icy Galilean satellites, *Icarus*, **149**, 133-159, 2001.
17. Cravens, T.E., C.N. Keller, and B. Ray, Photochemical sources of non-thermal neutrals for the exosphere of Titan, *Plant. Space Sci.,* **45**, 889, 1997.
18. Curtis, S.A., R.P. Lepping and E.C. Sittler Jr., The centrifugal flute instability and the generation of Saturnian kilometric radiation, *J. Geophys. Res.,* **91**, 10,989-10,994, 1986.
19. Delitsky, M. L. and A. L. Lane, Saturn's inner satellites: Ice chemistry and magnetospheric effects, *J. Geophys. Res.*, **107(E11)**, 5093, 2002.
20. Eviatar, A., R. L. McNutt, Jr., G.L. Siscoe and J.D. Sullivan, Heavy ions in the outer Kronian magnetosphere, *J. Geophys. Res.,* **88**, 823-831, 1983.
21. Eviatar, A. and M. Podolak, Titan's gas and plasma torus, *J. Geophys. Res.,* **88**, 833-840, 1983.
22. Fillius, W., W. H. Ip and C. E. McIlwain, Trapped radiation belts of Saturn: First Look, *Science*, **207**, 425, 1980.
23. Fillius, W. and C. E. McIlwain, Very energetic protons in Saturn's radiation belt, *J. Geophys. Res.*, **85**, 5803, 1980.
24. Galand, M., J. Lilensten, D. Toublanc and S. Maurice, The ionosphere of Titan: Ideal diurnal and nocturnal cases, *Icarus*, **140**, 92, 1999.
25. Gehrels, N., and E. C. Stone, Energetic oxygen and sulfur ions in the Jovian magnetosphere and their contribution to the auroral excitation, *J. Geophys. Res.*, **88(A7)**, 5537-5550, 1983.
26. Gobet, F. et al., Total partial and electron-capture cross-section for ionization of water vapor by 20-150 keV protons, *Phys. Rev.*, **86**, 3751-3754, 2001.
27. Goertz, C.K., Detached plasma in Saturn's turbulence layer, *Geophys. Res. Lett.*, **10**, 455, 1983.
28. Hartle, R.E., E.C. Sittler Jr., K. W. Ogilvie, J. D. Scudder, A.J. Lazarus and S. K. Atreya, Titan's ion exosphere observed from Voyager 1, *J. Geophys. Res.*, **87**, 1383, 1982.
29. Hill, T.W., Corotation lag in Jupiter's magnetosphere: Comparison of observation and theory, *Science,* **207**, 301-302, 1980.
30. Hunten, D.M., Thermal and nonthermal escape mechanisms for terrestrial bodies, *Planet. Space Sci.,* **30**, 773, 1982.
31. Hunten, D.M., M.G. Tomasko, F.M. Flaser, R.E. Samuelson, D.E. Strobel, et al., Titan, in *Saturn*, eds. T. Gehrels and M.S. Mathews, Univ. of Arizona Press, 671, 1984.
32. Ip, W.-H., Titan's ionosphere, *Astrophys. J.,* **362**, 354, 1990.
33. Ip, W., -H., The nitrogen tori of Titan and Triton, *Adv. Space Res.*, **12**, (8)73, 1992.
34. Johnson, R.E., Plasma-induced sputtering of an atmosphere, *Space Science Reviews*, **69**, 215-253, 1994.
35. Johnson, R. E., Pospieszalska, M. K., Sieveka, E. M., Cheng, A. F., Lanzerotti, L. J., and Sittler, E. C., "The Neutral Cloud and Heavy Ion Inner Torus at Saturn," *Icarus,* **77,** 311-329, 1989.

36. Johnson, R.E., M. Liu and C. Tully, Collisional dissociation cross-sections for O + O_2, CO and N_2, O_2 + O_2, N + N_2, and N_2 + N_2, *Planetary and Space Science,* **50**, 123, 2002.
37. Johnson, R.E., R.W. Carlson, J.F. Cooper, C. Paranicas, M.H. Moore, and M.C. Wong, "Radiation Effects on the Surface of the Galilean Satellites", *In Jupiter-The Planet, Satellites and Magnetosphere*, Ed. F. Bagenal, T. Dowling, and W.B. McKinnon, *Cambridge University, Combridge* in press, 2004.
38. Jurac, S., R. E. Johnson, and J. D. Richardson, Saturn's E ring and production of the neutral torus, *Icarus*, **149**, 384, 2001.
39. Keller, C. N., T. E. Cravens and L. Gan, A model of the ionosphere of Titan, *J. Geophys. Res.*, **97**, 12,117, 1992.
40. Keller, C. N., V. G. Anicich and T. E. Cravens, Model of Titan's ionosphere with detailed hydrocarbon ion chemistry, *Planet. Space Sci.*, **46**, 1157-1174, 1998.
41. Kennel, C.F. and H.E. Petschek, Limit on stably trapped fluxes, *J. Geophys. Res.,* **71**, 1, 1966.
42. Krimigis, S.M., T.P. Armstrong, W.I. Axford, C.O. Bostrom, C.Y. Fan, G. Gloeckler and L.J. Lanzerotti, The low energy charged particle (LECP) experiment on the Voyager spacecraft, *Space Sci. Rev.*, **21**, 329, 1977.
43. Krimigis, S.M., J.F. Carbary, E.P. Keath, C.O. Bostrom, W.I. Axford, G. Gloeckler, L.J. Lanzerotti and T.P. Armstrong, Characteristics of hot plasma in the Jovian magnetosphere: Results from the Voyager spacecraft, *J. Geophys. Res.,* **86**, 8227, 1981.
44. Krimigis, S. M., J. F. Carbary, E. P. Keath, T. P. Armstrong, L. J. Lanzerotti, and G. Gloeckler, General characteristics of hot plasma and energetic particles in the Saturnian magnetosphere: Results from the Voyager spacecraft, *J. Geophys. Res.*, **88**, 8871, 1983.
45. Krimigis, S. M., et al., Magnetospheric Imaging Instrument (MIMI) on the Cassini mission to Saturn/Titan, *Space Sci. Rev.*, in press, 2004.
46. Lammer, H. and S.J. Bauer, Atmospheric mass loss from Titan by sputtering, *Planet. Space Sci.,* **41**, 657, 1993.
47. Lazarus, A. J. and R. L. McNutt Jr., Low energy plasma ion observations in Saturn's magnetosphere, *J. Geophys. Res.*, **88**, 8831, 1983.
48. Lepping, R. P., W. H. Mish, E. C. Sittler, Jr. and S. A. Curtis, Analysis of waves in Saturn's magnetosphere: Voyager 1 observations, *NASA Tech. Memo., xxxxx*, 1986.
49. Lepping, R. P., W. H. Mish, E. C. Sittler, Jr., S. A. Curtis and B. T. Tsurutani, Analysis of waves in Saturn's magnetosphere: Voyager 1 observations, *J. Geophys. Res.*, submitted, 2004.
50. Lo, H. H., et al., Electron capture and loss collisions of heavy ions with atomic oxygen, *Phys. Rev.*, **A4**, 1462-1476, 1971.
51. Luna, H., M. Michael, M. B. Shah, R. E. Johnson, C. J. Latimer and J. W. McConkey, Dissociation of N_2 in capture and ionization collisions with fast H^+ and N^+ ions and modeling of positive ion formation in the Titan atmosphere, *J. Geophys. Res.*, **108**, xx, 2003.

52. Maclennan, C.G., L. J. Lanzerotti, S. M. Krimigis, R. P. Lepping and N. F. Ness, Effects of Titan on trapped particles in Saturn's magnetosphere, *J. Geophys. Res.*, **87**, 1411, 1982.
53. Mathie, R. A. and I. R. Mann, A correlation between extended intervals of ULF wave power and storm-time geosynchronous relativistic electron flux enhancements, *Geophys. Res. Lett.*, **27**, 3261-3264, 2000.
54. Maurice, S., E. C. Sittler Jr., J. F. Cooper, B. H. Mauk, M. Blanc, and R. S. Selesnick, Comprehensive analysis of electron observations at Saturn: Voyager 1 and 2, *J. Geophys. Res.*, **101**, 15211, 1996.
55. McClure, G.W., Electron transfer in proton-hydrogen-atom collision: 2-117 keV, *Phys. Rev.*, **148**, 47-54, 1966.
56. McDonough, T. R. and N. M. Brice, A Saturnian gas ring and recycling of Titan's atmosphere, *Icarus*, **20**, 136-145, 1973.
57. McIlwain, C. E., Substorm injection boundaries, In *Magnetospheric Physics*, edited by B. M. McCormac, D. Reidel, Hingham, Mass., 143, 1974.
58. McPherron, R. L., The role of substorms in the generation of magnetic storms, *Magnetic Storms*, Eds. B. T. Tsurutani, W. D. Gonzalez, Y. Kamide, J. K. Arballo, Geophysical Monograph 98, 131, 1997.
59. McPherron, R. L., D. N. Baker and L. F. Bargatze, Linear filters as a method of real time prediction of geomagnetic activity, Terra Scientific Publishing Co. (Tokyo), 85-92, 1986.
60. Michael, M. and R.E. Johnson, Nitrogen emissions from Titan due to energetic electron bombardment, manuscript, 2003.
61. Moore, M. H. and R. L. Hudson, IR detection of H_2O_2 at 80 K in ion-irradiated laboratory ices relevant to Europa, *Icarus*, **145**, 282-288, 2000.
62. Morrison, D., T. V. Johnson, E. M. Shoemaker, L. A. Soderblom, P. Thomas, J. Veverka and B. A. Smith, Satellite of Saturn: Geological perspective, in *Saturn*, edited by T. Gehrels and M. S. Matthews, Univ. of Ariz. Press, Tucson, 1984.
63. Neubauer, F.M., D.A. Gurnett, J.D. Scudder, and R.E. Hartle, Titan's magnetospheric interaction, in *Saturn,* eds. T. Gehrels and M.S. Matthews, Univ. of Arizona Press, Tucson, 571, 1984.
64. Noll, K. S., T. Rousch, D. Cruikshank and R. E. Johnson, Detection of ozone on Saturn's satellites Dione and Rhea, *Nature*, **388**, 45, 1997.
65. Paonessa, M. T. and A. F. Cheng, A theory of satellite sweeping, *J. Geophys. Res.*, **90**, 3428-3434, 1985.
66. Paonessa, M. T. and A. F. Cheng, Limits on ion radial diffusion coefficients in Saturn's inner magnetosphere, *J. Geophys. Res.,* **91**, 1391-1396, 1986.
67. Paranicas, C. and A. F. Cheng, A model of satellite microsignatures for Saturn, Icarus, 125, 380, 1997.
68. Paranicas, C., A. F. Cheng, B. H. Mauk, E. P. Keath and S. M. Krimigis, Evidence of a source of energetic ions at Saturn, *J. Geophys. Res.*, **102**, 17,459-17,466, 1997.
69. Paranicas, C., R. B. Decker, B.H. Mauk, S.M. Krimigis, T.P. Armstrong and S. Jurac, *Geophys. Res. Lett.*, submitted, 2004.

70. Phaneuf, R.A., et al., Single-electron capture by multiply charge ions of carbon, nitrogen and oxygen in atomic and molecular hydrogen, *Phys. Rev.*, **A4**, 534-545, 1978.
71. Randall, B. A., Energetic electrons in the magnetosphere of Saturn, *J. Geophys. Res.*, **99**, 8771, 1994.
72. Richardson, J. D., Thermal ions at Saturn: Plasma parameters and implications, *J. Geophys. Res.*, **91**, 1381, 1986.
73. Richardson, J. D., A. Eviatar, M. A. McGrath, and V. M. Vasyliunas, OH in Saturn's magnetosphere: Observations and implications, *J. Geophys. Res.*, **103**, 20245, 1998.
74. Sandel, B.R. and A.L. Broadfoot, Morphology of Saturn's aurora, *Nature (London)*, **292**, 679-682, 1981.
75. Sandel, B.R., D.E. Shemansky, A.L. Broadfoot, J.B. Holberg, G.R. Smith, J.C. McConnell, D.F. Strobel, S.K. Atreya, T.M. Donahue, H.W. Moos, D.M. Hunten, R.B. Pomphrey and S. Linick, Extreme ultraviolet observations from the Voyager 2 encounter with Saturn, *Science,* **215**, 548-553, 1982.
76. Scarf ,F.L., L.A. Frank, D.A. Gurnett, L.J. Lanzerotti, A. Lazarus and E.C. Sittler, Jr., Measurement of plasma, plasma waves, and suprathermal charged particles in Saturn's inner magnetosphere, , in *Saturn*, eds. T. Gehrels and M.S. Mathews, Univ. of Arizona Press, 318, 1984.
77. Schardt, A. W. and F. B. McDonald, The flux and source of energetic protons in Saturn's inner magnetosphere, *J. Geophys. Res.*, **88**, 8923, 1983.
78. Schultz, M. and L.J. Lanzerotti, Particle Diffusion in the Radiation Belts, *Physics and Chemistry in Space 7, Springer-Verlag*, 1974.
79. Shemansky, D. E. and D. T. Hall, The distribution of atomic hydrogen in the magnetosphere of Saturn, *J. Geophys. Res.*, **97**, 4143-4161, 1992.
80. Shemansky, D. E., P. Matherson, D. T. Hall, H.-Y. Hu and T. M. Tripp, Detection of the hydroxyl radical in the Saturn magnetosphere, *Nature*, **363**, 329-332, 1993.
81. Shemantovich, V.I., Kinetic modeling of suprathermal nitrogen atoms in the Titan's atmosphere: I. Sources, *Solar System Research,* **32**, 384, 1998.
82. Shemantovich, V.I., Kinetic modeling of suprathermal nitrogen atoms in the Titan's atmosphere: II. Escape flux due to dissociation processes, *Solar System Research,* **33**, 32, 1999.
83. Shematovich, V.I., C. Tully and R.E. Johnson, Suprathermal nitrogen atoms and molecules in Titan's corona, *Adv. Space Res.,* **27**, 1875-1880, 2001.
84. Shematovich, V.I., R.E. Johnson, M. Michael and J.G. Luhmann, Nitrogen loss from Titan, manuscript in preparation, 2003.
85. Siscoe, G. L., N. F. Ness and C. M. Yeates, Substorms on Mercury?, *J. Geophys. Res.*, **80**, 4359, 1975.
86. Sittler, E. C., Jr., K. W. Ogilvie and J. D. Scudder, Survey of low energy plasma electrons in Saturn's magnetosphere: Voyager 1 and 2, *J. Geophys. Res.*, **88**, 8847, 1983.
87. Sittler, E.C., Jr.,R.E. Johnson, S. Jurac, J.D. Richardson, M. McGrath ,F. Crary, D. Young and J.E. Nordholt, Pickup ions at Dione and Enceladus: Cassini Plasma Spectrometer Simulations, *J. Geophys. Res.,* **109**, A01214, 2004a.

88. Sittler, E. C., Jr., R. E. Hartle, A. F. Vinas, R. E. Johnson, H. T. Smith and I. Mueller-Wodard, Titan interaction with Saturn's magnetosphere: Mass loading and ionopause location, Titan Symposium at ESTEC, J. P. Lebreton Editor, 2004b.
89. Slavin, J. A. and R. E. Holzer, The effect of erosion on the solar wind stand-off distance at Mercury, *J. Geophys. Res.*, **84**, 2076, 1979.
90. Smith, E. J., L. Davis Jr., D. E. Jones, P. J. Coleman, Jr., D. S. Colburn, P. Dyal and C. P. Sonett, Saturn's magnetosphere and its interaction with the solar wind, *J. Geophys. Res.*, **85**, 5655, 1980.
91. Smith, E.J. and B. T. Tsurutani, Saturn's magnetosphere: Observations of ion cyclotron waves near the Dione L shell, *J. Geophys. Res.*, **88**, 7831, 1983.
92. Smith, H. T., R. E. Johnson and V. Shemantovich, Titan's atomic and molecular nitrogen tori, *Geophys. Res. Lett.*, 2004GL020580, 2004.
93. Sonnerup, B. U. and K. D. Siebert, Theory of the low latitude boundary layer and its coupling to the ionosphere: A tutorial review, *Earth's Low-Latitude Boundary Layer*, Eds. P. T. Newell and T. Onsager, American Geophysical Union Press, **133**, 13-32, 2003.
94. Southward, D. J. and W. J. Hughes, Theory of hydrodynamic waves in the magnetosphere, *Space Sci. Rev.,* **35**, 301-366, 1983.
95. Stevenson, D.J., Volcanism and igneous processes in small icy satellites, *Nature*, **298**, 142, 1982.
96. Strazzulla, G., G. Leto, O. Gomis and M. A. Satorre, Implantation of carbon and nitrogen ions in water ice, *Icarus*, **164**, 163-169, 2003.
97. Strobel, D.F. and D.E. Shemansky, EUV emission from Titan's upper atmosphere: Voyager 1 encounter, *J. Geophys. Res.*, **87**, 1361-1368, 1982.
98. Strobel, D.F., M.E. Summers and X. Zhu, Titan's upper atmosphere: Structure and ultraviolet emissions, *Icarus,* **100**, 512, 1992.
99. Summers, D., R. M. Thorne and F. Xiao, Relativistic theory of wave-particle resonant diffusion with application to electron acceleration in the magnetosphere, *J. Geophys. Res.*, **103**, 20,487-20,500, 1998.
100. Thompson, W.R., et al., One-electron capture in collisions of 6-100 keV protons with oxygen atoms, *J. Phys. B: At. Mol. Opt. Phys.*, **29**, 725-732, 1996.
101. Thomsen, M.F. and J.A. Van Allen, On the inference of properties of Saturn's ring E from energetic particle observations, *Geophys. Res. Lett.*, **6**, 893, 1979.
102. Thomsen, M. F. and J. A. Van Allen, Motion of trapped electrons and protons in Saturn's inner magnetosphere, *J. Geophys. Res.*, **85**, 5831, 1980.
103. Thorne, R.M., Microscopic plasma processes in the Jovian magnetosphere, *Physics of the Jovian Magnetosphere*, A.J. Dessler, Ed., 454, 1983.
104. Tsurutani, B.T. and G.S. Lakhina, Some basic concepts of wave-particle interactions in collisionless plasmas, *Rev. of Geophys.*, **35**, 491, 1997.
105. Tsurutani, B.T., X.Y. Zhou, V.M. Vasyliunas, G. Haerendel, J.K. Arballo and G.S. Lakhina, Interplanetary shocks, magnetopause boundary layers and dayside auroras: The importance of a very small region, *Surveys in Geophysics*, **22**, 101, 2001.

106. Tsurutani, B.T., G.S. Lakhina, L. Zhang, J.S. Pickett and Y. Kasahara, ELF/VLF plasma waves in the Low Latitude Boundary Layer, *in Earth's Low Latitude Boundary Layer*, edited by P. Newell and T. Onsager, American Geophysical Union Press, **133**, 189, 2003.

107. Tully, C. and R. E. Johnson, Semiclassical calculation of collisional dissociation cross sections for $N+N_2$, *J. of Chemical Physics*, **117**, 6556, 2002.

108. Van Allen, J. A., B. A. Randall and M. F. Thomsen, Sources and sinks of energetic electrons and protons in Saturn's magnetosphere, *J. Geophys. Res.*, **85**, 5679, 1980.

109. Vasyliunas, V.M., Mathematical models of magnetospheric convection and its coupling to the ionosphere, In *Particles and Fields in the Magnetosphere*, ed. B. M. McCormac, D. Reidel, Dordrecht, Netherlands, 60-71, 1970.

110. Vasyliunas, V. M., Concepts of magnetospheric convection, In *The Magnetospheres of the Earth and Jupiter*, ed. V. Formisano, D. Reidel, Dordrecht, 179-188, 1975.

111. Vasyliunas, V.M. and G.L. Siscoe, On the flux and the energy spectrum of interstellar ions in the solar system, *J. Geophys. Res.*, **81**, 1247, 1976a.

112. Vasyliunas, V. M., An overview of magnetospheric dynamics, In *Magnetospheric Particle and Fields*, ed. B. M. McCormac, D. Reidel, Dordrecht, 99-110, 1976b.

113. Warwick, J.W., J.B. Pierce, D.R. Evans, T.D. Carr, J.J. Schauble, J.K. Alexander, M.L. Kaiser, M.D. Desch, M. Pedersen, A. Lecacheux, G. Daigne, A. Boischot and C.H. Barrow, Planetary radio astronomy observations from Voyager 1 near Saturn, *Science,* **212**, 239-243, 1981.

114. Young, D. T., et al., Cassini Plasma Spectrometer, *Space Sci. Rev.*, in press, 2004.

115. Ziegler, J. F., J. P. Biersack, and U. Littmark, *The Stopping and Range of Ions in Solids*. Pergamon Press, New York, 1985.

Figure Captions

Figure 1. (a) A 2D Monte Carlo calculation of Titan's atomic nitrogen torus assuming a sputtered source with source strength of $S_N \sim 4.5x10^{25}$ N/s, an energy spectrum characteristic of sputtered neutrals, spectral parameter U ~ 0.3 eV and lifetime of atomic nitrogen within Saturn's magnetosphere of $\tau_{N0} \sim 3x10^7$ sec. (b) Same as (a), except monoenergetic lanching energy with speed ~ 1 km/s is used. See text for details.

Figure 2. Voyager 1 PLS plasma ion data observed within Titan's atomic neutral torus near the ring plane. A three-component Maxwellian spectrum was fit to the data where the presence of a heavy suprathermal component is clearly evident.

Figure 3. Voyager 2 PLS plasma ion data observed near Titan's L shell, but at high latitudes, well above the ring plane. Interference in sensor's A, B and C is present at the higher ion energies which makes interpretation of this data difficult. But, it is felt that the measurements in the D cup are of good quality and shows no evidence of a suprathermal component. This interpretation is based on a survey of such measurements within Saturn's outer magnetosphere where the Titan nitrogen torus is expected to reside.

Figure 4. A combined plot of Voyager 1 PLS and LECP ion data within the Titan torus during the spacecraft inbound pass of Saturn's magnetosphere. For the thermal ions we used H^+ and O^+, while the suprathermal component for PLS was assumed to be N^+. For the LECP data we assumed N^+. In the case of the ion data labeled as PLS, we have interpolated the intensities from 5 keV to 10 keV. We have also super-imposed the Voyager 1 and 2 electron data from PLS and LECP. The CRS (Cosmic Ray Detector System) fluxes in this outer region went undetected. We have combined the Voyager 1 and electron data, since the Voyager 1 LECP instrument had its gamma detectors turned off, while they were on for Voyager 2. The high energy electron data was less latitudinal dependent, but this is not the case for the thermal electrons (i.e., plasma centrifugally confined). The particle fluxes have been converted into intensities.

Figure 5. Here we show the loss of ions via satellite sweeping at Rhea's L shell for a range of radial diffusion coefficients. The calculations assumed either all protons or all nitrogen ions. When the transport time scales $\tau \sim 10$ days nitrogen ions are enriched relative to protons as they diffuse radially inward across Rhea's L shell. For time scales $\tau \sim 1$ day and $\tau \sim 100$ days no enrichment of N^+ relative to protons occurs.

Figure 6. TRIM code calculation of stopping range for H, He, C, N and O in ice are shown as a function of particle incident energy. These calculations can be used for calculations of ion loss due to interaction with ring material composed of ice.

Figure 7. Plot of relevant time scales for Saturn's magnetosphere: radial diffusion, wave scattering, and satellite sweeping. See text for details.

Figure 8. Voyager 1 PLS ion spectrum measured during the Dione ring plane crossing. A three-component Maxwellian fit was performed with H^+ and O^+ used for the thermal component and H^+ used for the suprathermal component. The presence of a suprathermal ion component is clearly evident. This fit shows that protons provide a poor fit to the suprathermal component. This is clearly evident in the D cup measurements.

Figure 9. The same as Figure 8, except N^+ is now used instead of protons. Here, because of a Mach number effect, the fit is considerably improved. It is felt that by using a shell distribution we would get a better fit to the A, B and C sensors. But, this needs to be confirmed by more quantitative calculations where a shell distribution is assumed for the suprathermal component.

Figure 10. A combined plot of PLS and LECP ion data recorded during the Voyager 1 ring plane crossing at Dione's L shell. For PLS we have assumed H^+ and O^+ for the thermal ions and O^+ for the suprathermal ions. For the LECP data we have assumed N^+ ions. In the case of the ion data labeled as PLS, we have interpolated the intensities from 5 keV to 10 keV. We have also super-imposed the Voyager 1 and 2 electron data from PLS, LECP and CRS (Cosmic Ray Detector System). We have done this since the Voyager 1 LECP instrument had its gamma detectors turned off, while they were on for Voyager 2. The high energy electron data was less latitudinal dependent, but this is not the case for the thermal electrons (i.e., plasma centrifugally confined). The particle data has been converted into intensities.

Figure 11. Using the data in Figure 10 and assuming N^+ ions for $E > 10$ keV, we have computed the ion implantation rates as a function of depth for H^+, O^+ and N^+ within the icy surface of the moon Dione. See text for details.

Figure 12. Similar to that done for Figure 11, we have computed the dosage time scales for radiolysis as a function of depth in the icy surface of Dione. This figure shows the time scales at which radiolytic chemistry can occur as a function of depth in the ice.

Figure 13. Infrared spectrum of $H_2O + N_2 + O_2$ (3:1:1) at 20 K before and after irradiation with 0.8 MeV protons. The spectrum before irradiation shows small absorption features due to the forbidden transitions of both N_2 and O_2. After irradiation to a dose of ~ 4 eV (16 amu molecule)$^{-1}$, product molecules NO, NO_2, N_2O, O_3, and H_2O_2 are easily identified.

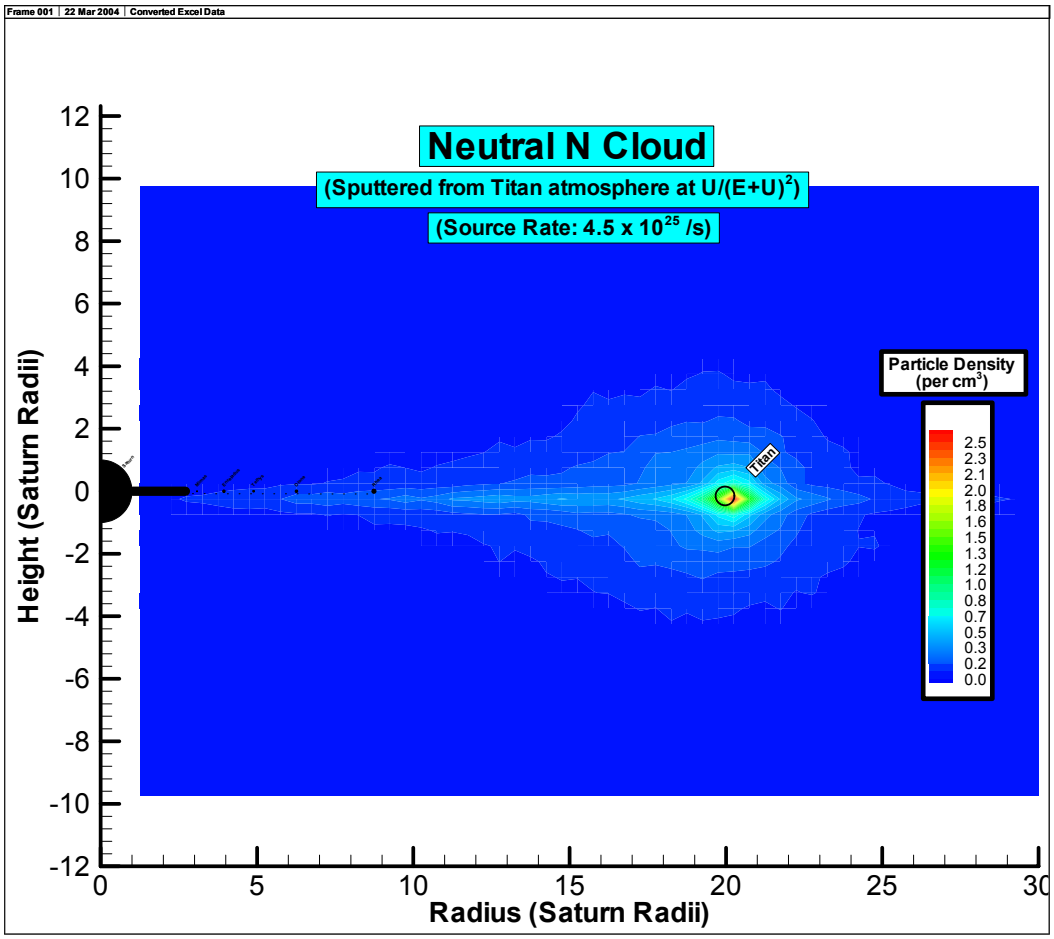
Frame 001 | 22 Mar 2004 | Converted Excel Data
Neutral N Cloud
(Sputtered from Titan atmosphere at U/(E+U)^2)
(Source Rate: 4.5 x 10^{25} /s)
Particle Density (per cm^3)
2.5
2.3
2.1
2.0
1.8
1.6
1.5
1.3
1.2
1.0
0.8
0.7
0.5
0.3
0.2
0.0
Titan
Height (Saturn Radii)
12
10
8
6
4
2
0
-2
-4
-6
-8
-10
-12
0
5
10
15
20
25
30
Radius (Saturn Radii)

Figure 1a.

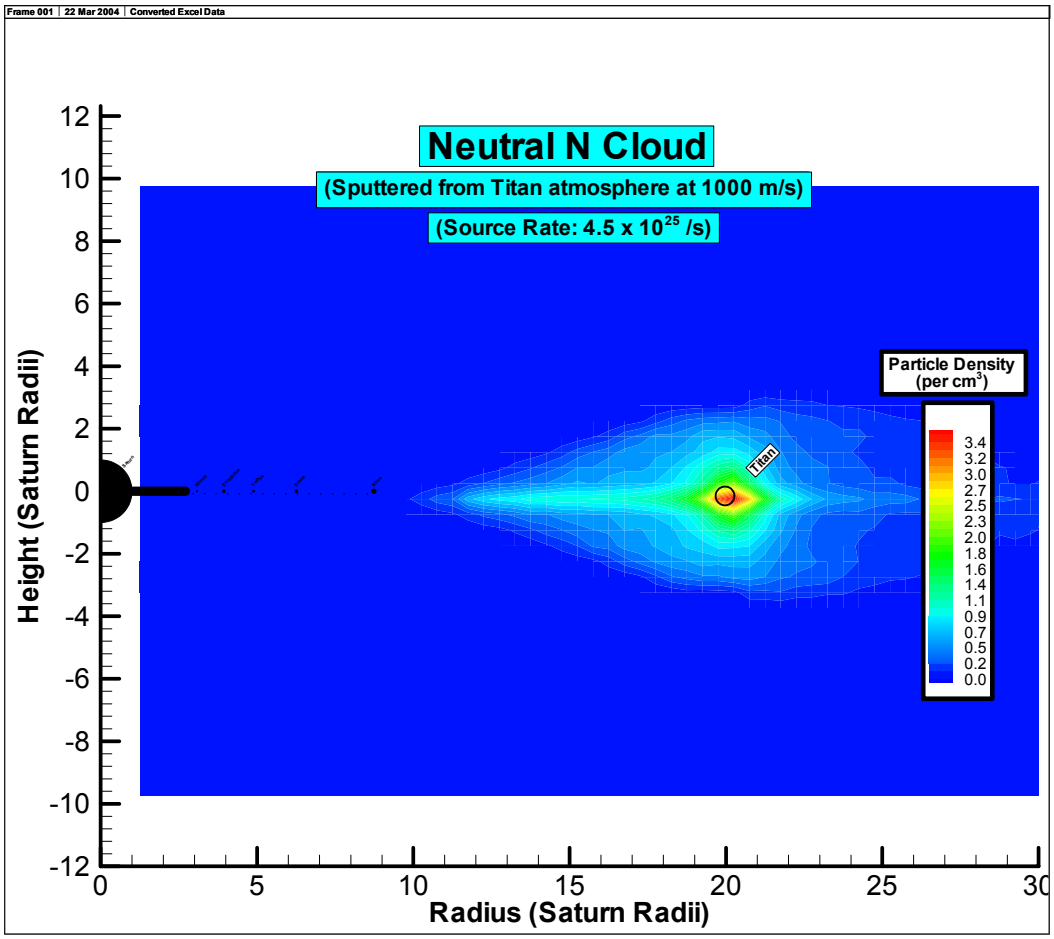
Frame 001 | 22 Mar 2004 | Converted Excel Data
Neutral N Cloud
(Sputtered from Titan atmosphere at 1000 m/s)
(Source Rate: 4.5 x 10^25 /s)
Particle Density (per cm^3)
3.4
3.2
3.0
2.7
2.5
2.3
2.0
1.8
1.6
1.4
1.1
0.9
0.7
0.5
0.2
0.0
Titan
Height (Saturn Radii)
12
10
8
6
4
2
0
-2
-4
-6
-8
-10
-12
0
5
10
15
20
25
30
Radius (Saturn Radii)

Figure 1b.

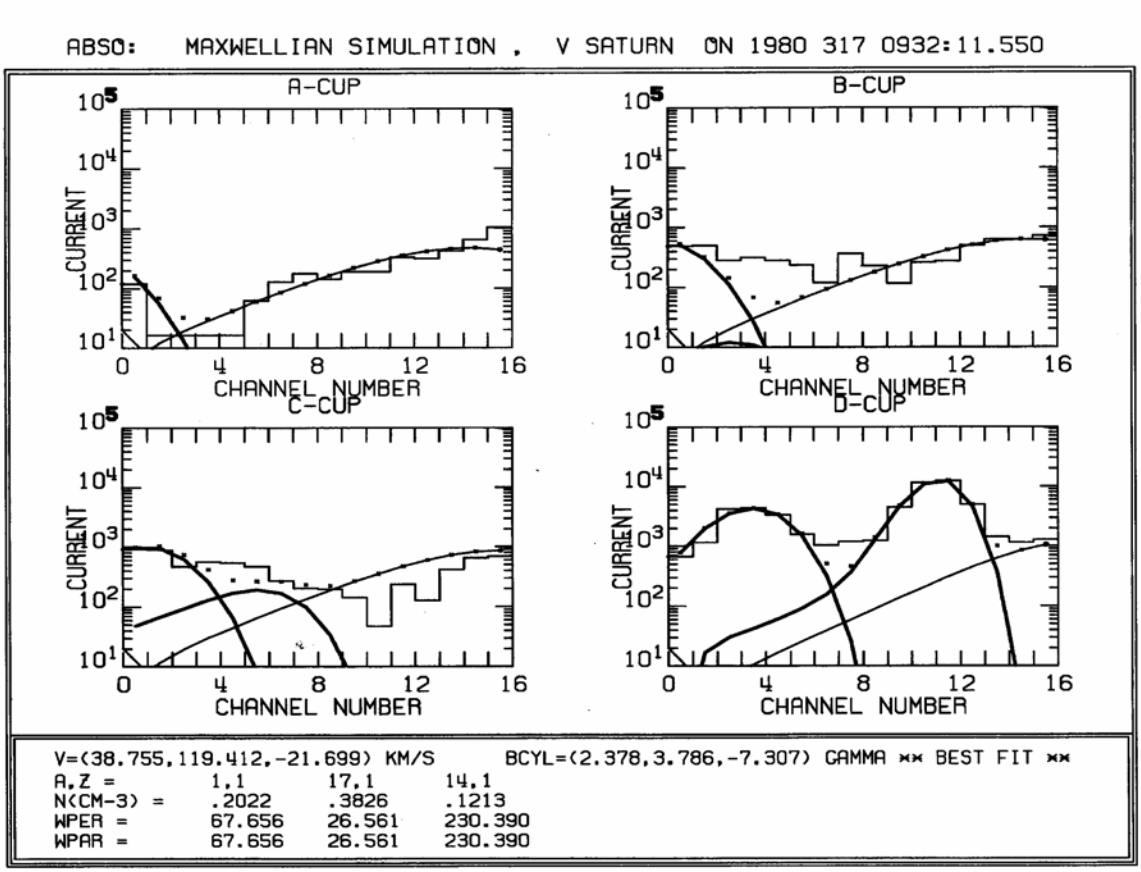
ABSO: MAXWELLIAN SIMULATION . V SATURN ON 1980 317 0932:11.550
A-CUP
B-CUP
C-CUP
D-CUP
CURRENT
CHANNEL NUMBER
V=(38.755,119.412,-21.699) KM/S
BCYL=(2.378,3.786,-7.307) GAMMA ** BEST FIT **
A,Z = 1,1 17,1 14,1
N(CM-3) = .2022 .3826 .1213
WPER = 67.656 26.561 230.390
WPAR = 67.656 26.561 230.390

Figure 2.

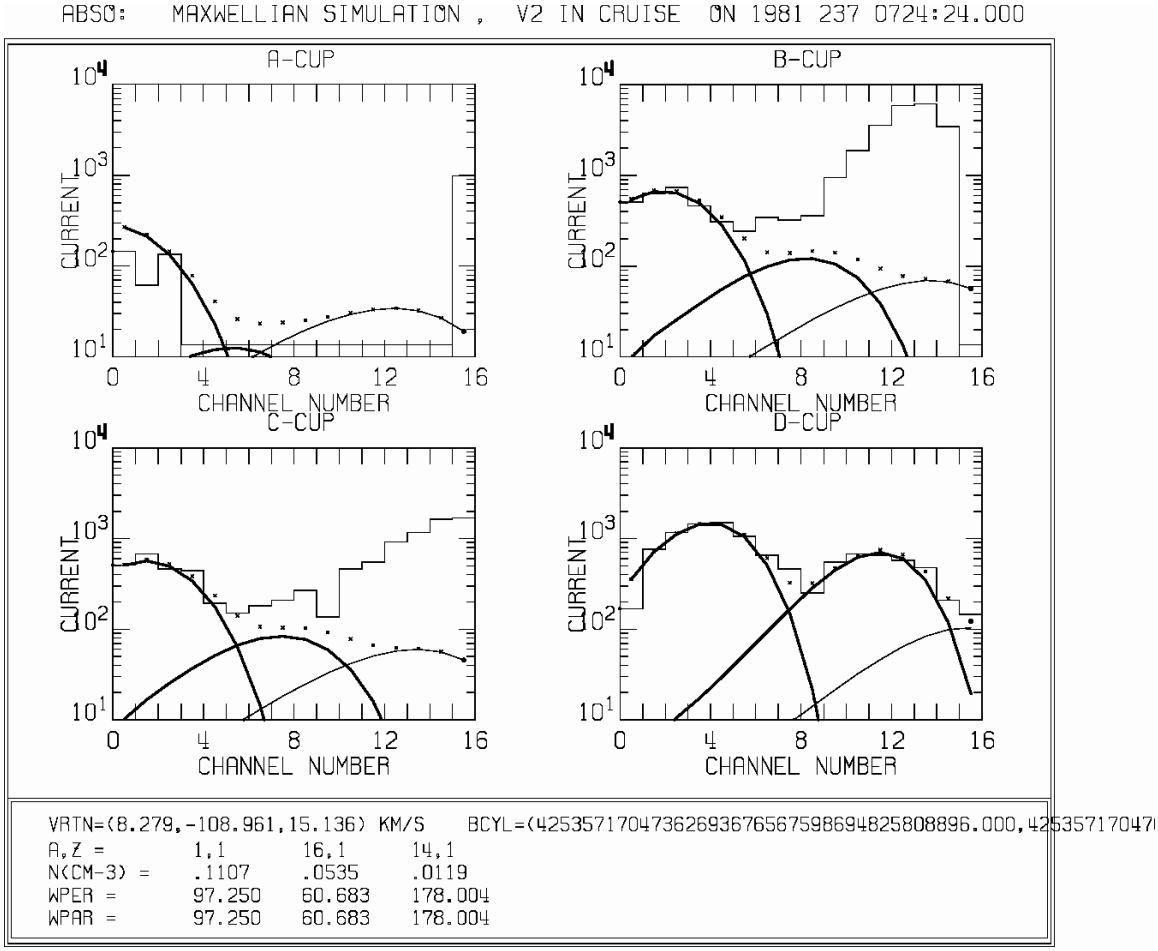
ABSO: MAXWELLIAN SIMULATION , V2 IN CRUISE ON 1981 237 0724:24.000
A-CUP
B-CUP
C-CUP
D-CUP
CURRENT
CHANNEL NUMBER
VRTN=(8.279,-108.961,15.136) KM/S
A,Z = 1,1 16,1 14,1
N(CM-3) = .1107 .0535 .0119
WPER = 97.250 60.683 178.004
WPAR = 97.250 60.683 178.004

Figure 3.

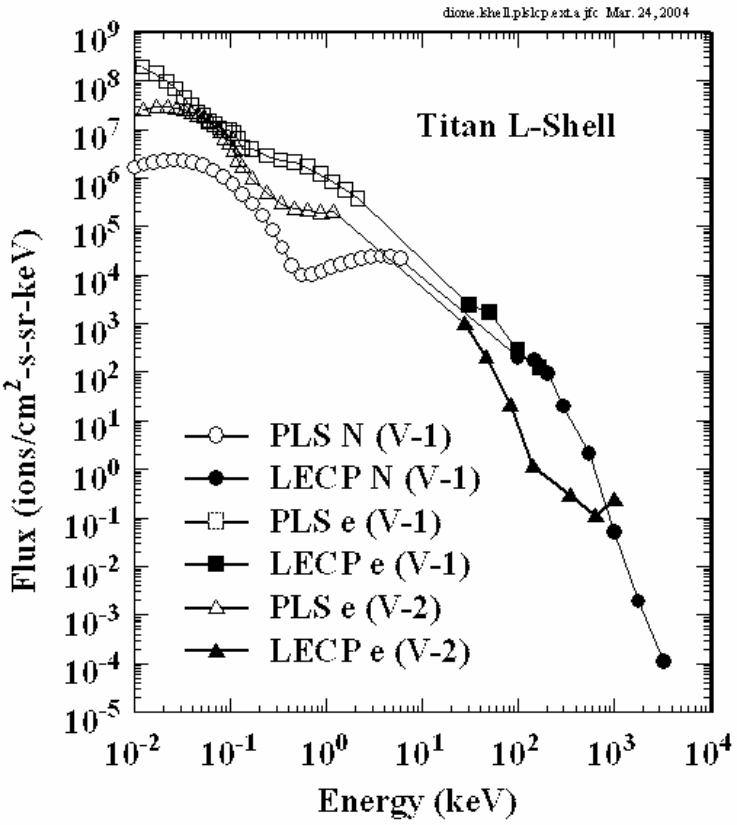
dione.khell.plslcp.extra.jfc Mar. 24, 2004
Titan L-Shell
PLS N (V-1)
LECP N (V-1)
PLS e (V-1)
LECP e (V-1)
PLS e (V-2)
LECP e (V-2)
Flux (ions/cm^2-s-sr-keV)
Energy (keV)
10^9
10^8
10^7
10^6
10^5
10^4
10^3
10^2
10^1
10^0
10^{-1}
10^{-2}
10^{-3}
10^{-4}
10^{-5}
10^{-2}
10^{-1}
10^0
10^1
10^2
10^3
10^4

Figure 4.

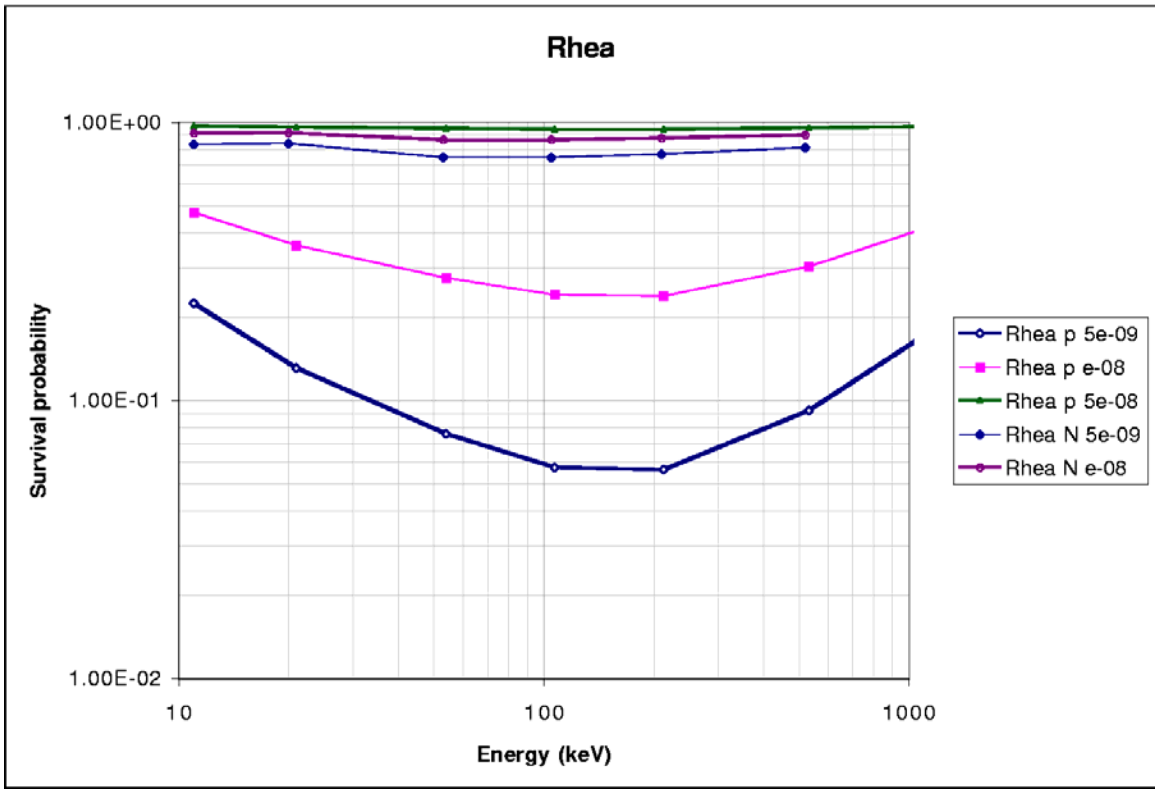
Rhea
1.00E+00
1.00E-01
1.00E-02
Survival probability
10
100
1000
Energy (keV)
Rhea p 5e-09
Rhea p e-08
Rhea p 5e-08
Rhea N 5e-09
Rhea N e-08

Figure 5.

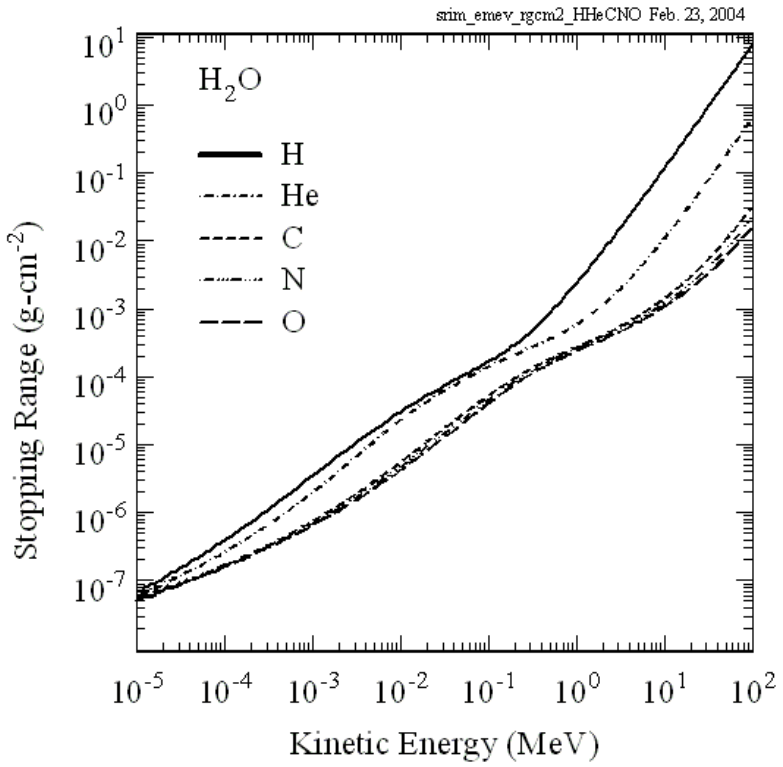
srim_emev_rgcm2_HHeCNO Feb. 23, 2004
H2O
H
He
C
N
O
Stopping Range (g-cm-2)
Kinetic Energy (MeV)
10^1
10^0
10^-1
10^-2
10^-3
10^-4
10^-5
10^-6
10^-7
10^-5
10^-4
10^-3
10^-2
10^-1
10^0
10^1
10^2

Figure 6.

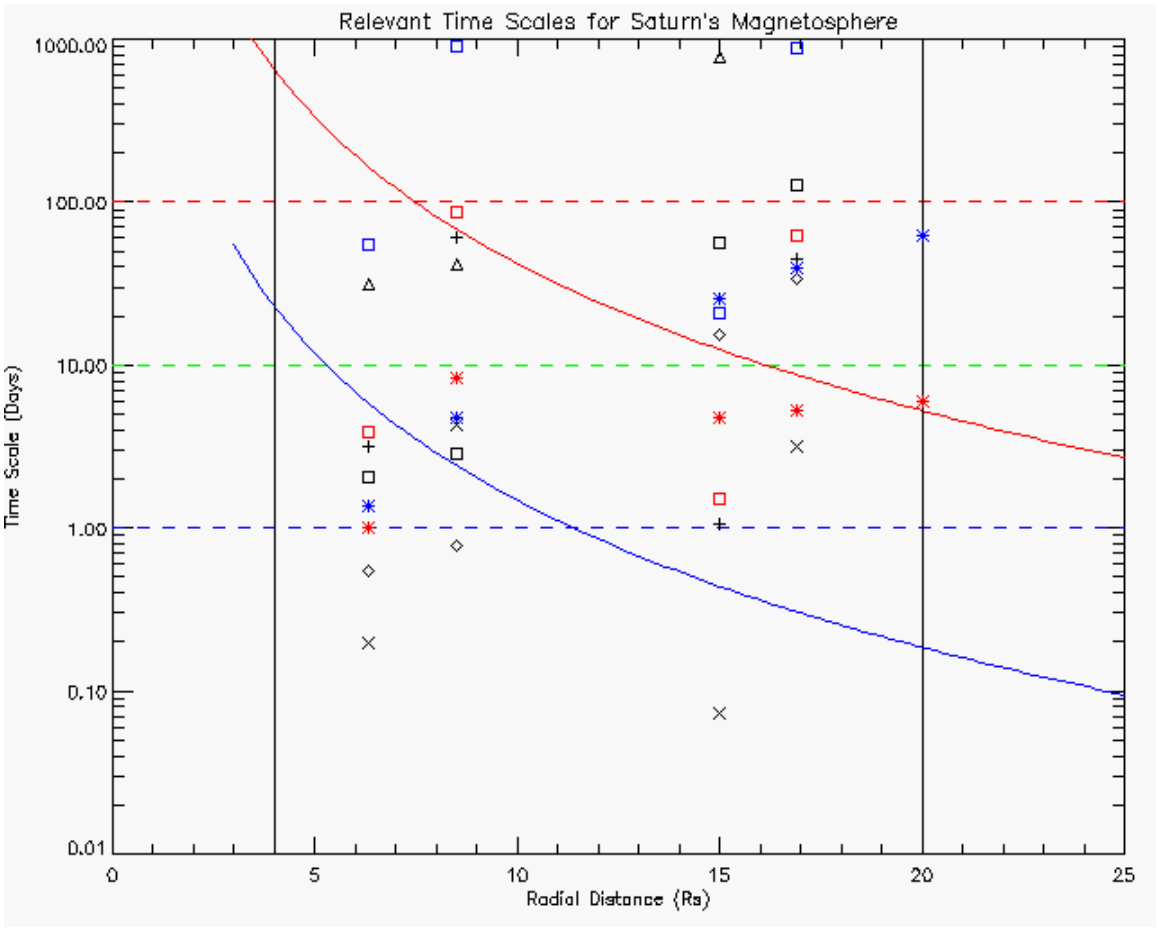
Relevant Time Scales for Saturn's Magnetosphere
1000.00
100.00
10.00
1.00
0.10
0.01
Time Scale (Days)
0
5
10
15
20
25
Radial Distance (Rs)

Figure 7.

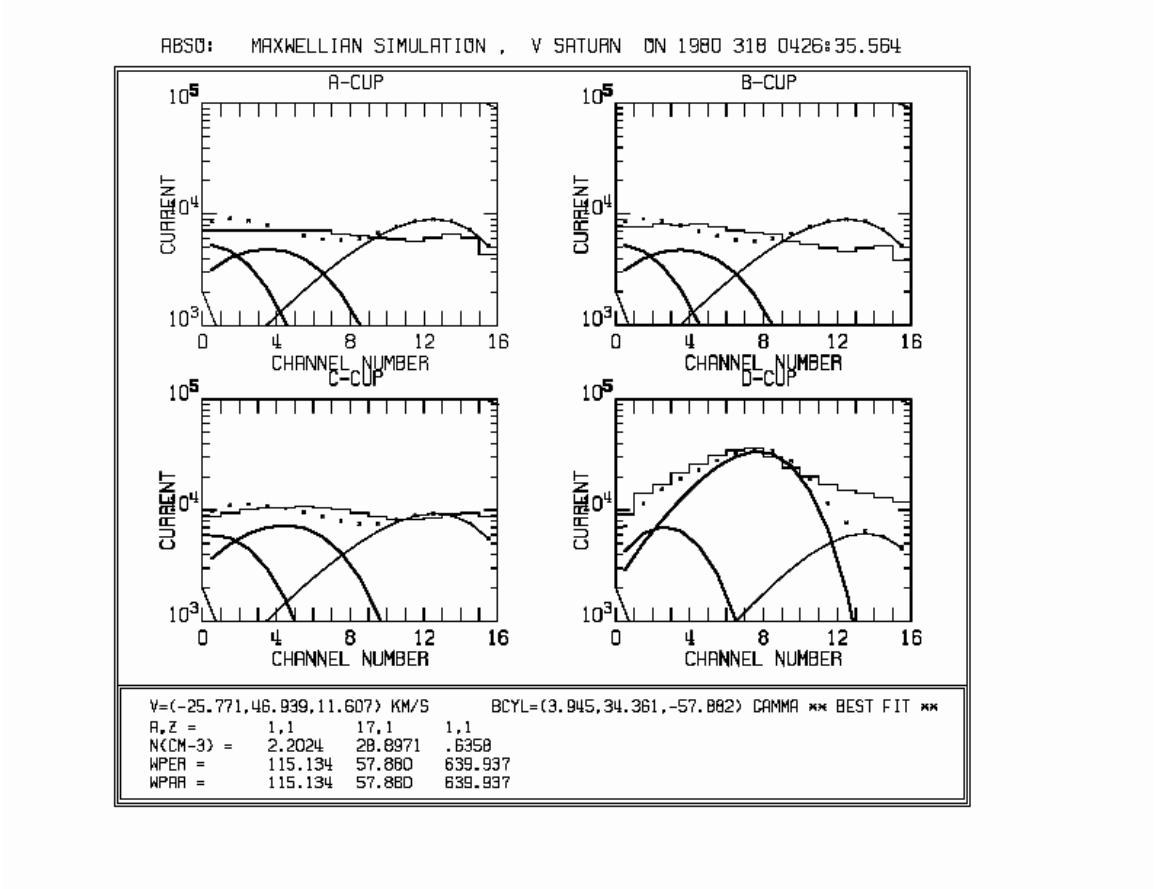
ABSO: MAXWELLIAN SIMULATION , V SATURN ON 1980 318 0426:35.564
A-CUP
B-CUP
C-CUP
D-CUP
CURRENT
CHANNEL NUMBER
V=(-25.771,46.939,11.607) KM/S
BCYL=(3.945,34.361,-57.882) GAMMA ** BEST FIT **
R,Z = 1,1 17,1 1,1
N(CM-3) = 2.2024 28.8971 .6358
WPER = 115.134 57.880 639.937
WPAR = 115.134 57.880 639.937

Figure 8.

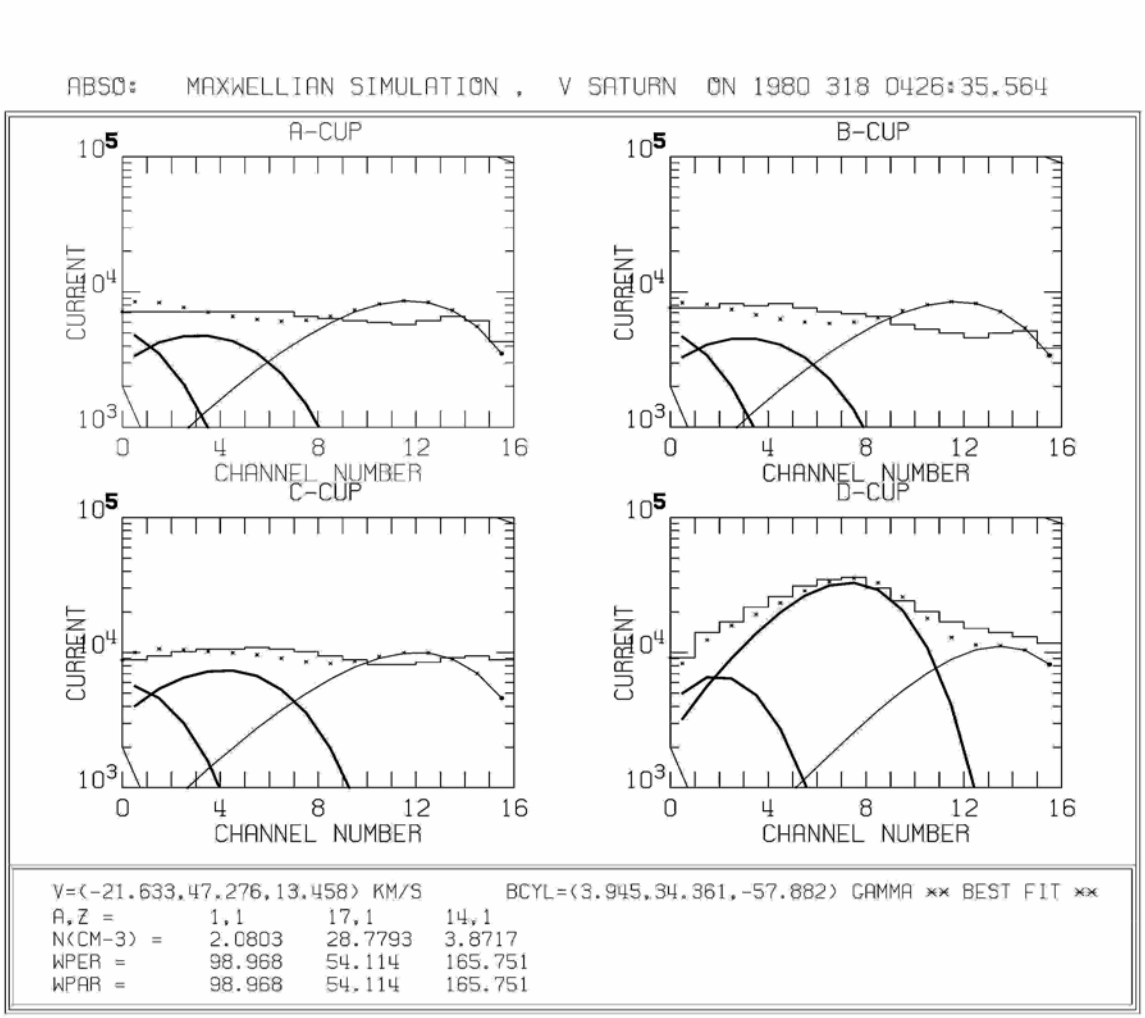
ABSO: MAXWELLIAN SIMULATION , V SATURN ON 1980 318 0426:35.564
A-CUP
B-CUP
C-CUP
D-CUP
CURRENT
CHANNEL NUMBER
V=(-21.633,47.276,13.458) KM/S
BCYL=(3.945,34.361,-57.882) GAMMA ** BEST FIT **
A,Z = 1,1 17,1 14,1
N(CM-3) = 2.0803 28.7793 3.8717
WPER = 98.968 54.114 165.751
WPAR = 98.968 54.114 165.751

Figure 9.

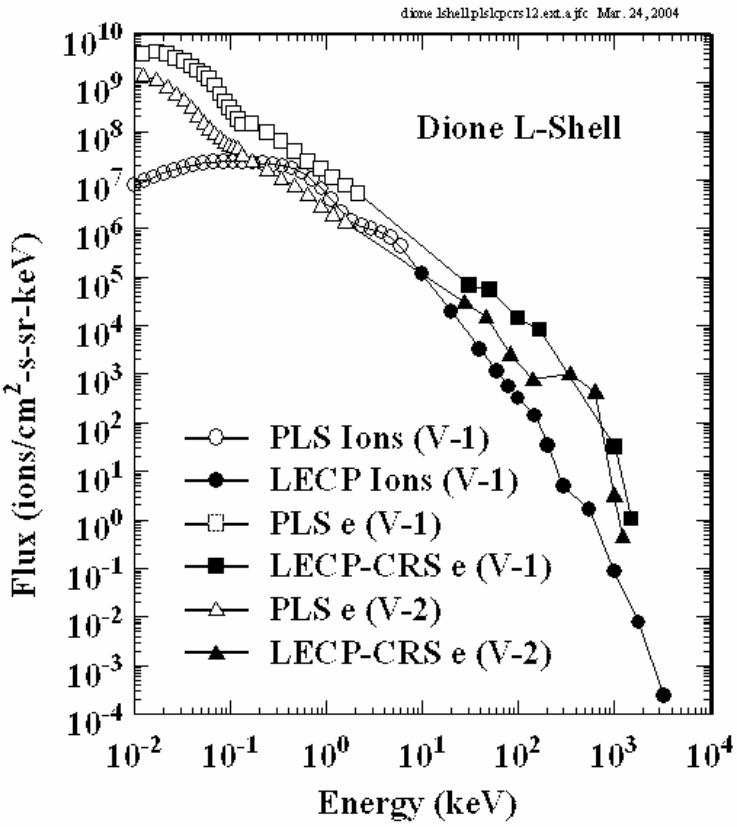
dione lshellplslcpcrs12.ext.a.jfc Mar. 24, 2004
Dione L-Shell
PLS Ions (V-1)
LECP Ions (V-1)
PLS e (V-1)
LECP-CRS e (V-1)
PLS e (V-2)
LECP-CRS e (V-2)
Flux (ions/cm^2-s-sr-keV)
Energy (keV)
10^{10}
10^{9}
10^{8}
10^{7}
10^{6}
10^{5}
10^{4}
10^{3}
10^{2}
10^{1}
10^{0}
10^{-1}
10^{-2}
10^{-3}
10^{-4}
10^{-2}
10^{-1}
10^{0}
10^{1}
10^{2}
10^{3}
10^{4}

Figure 10.

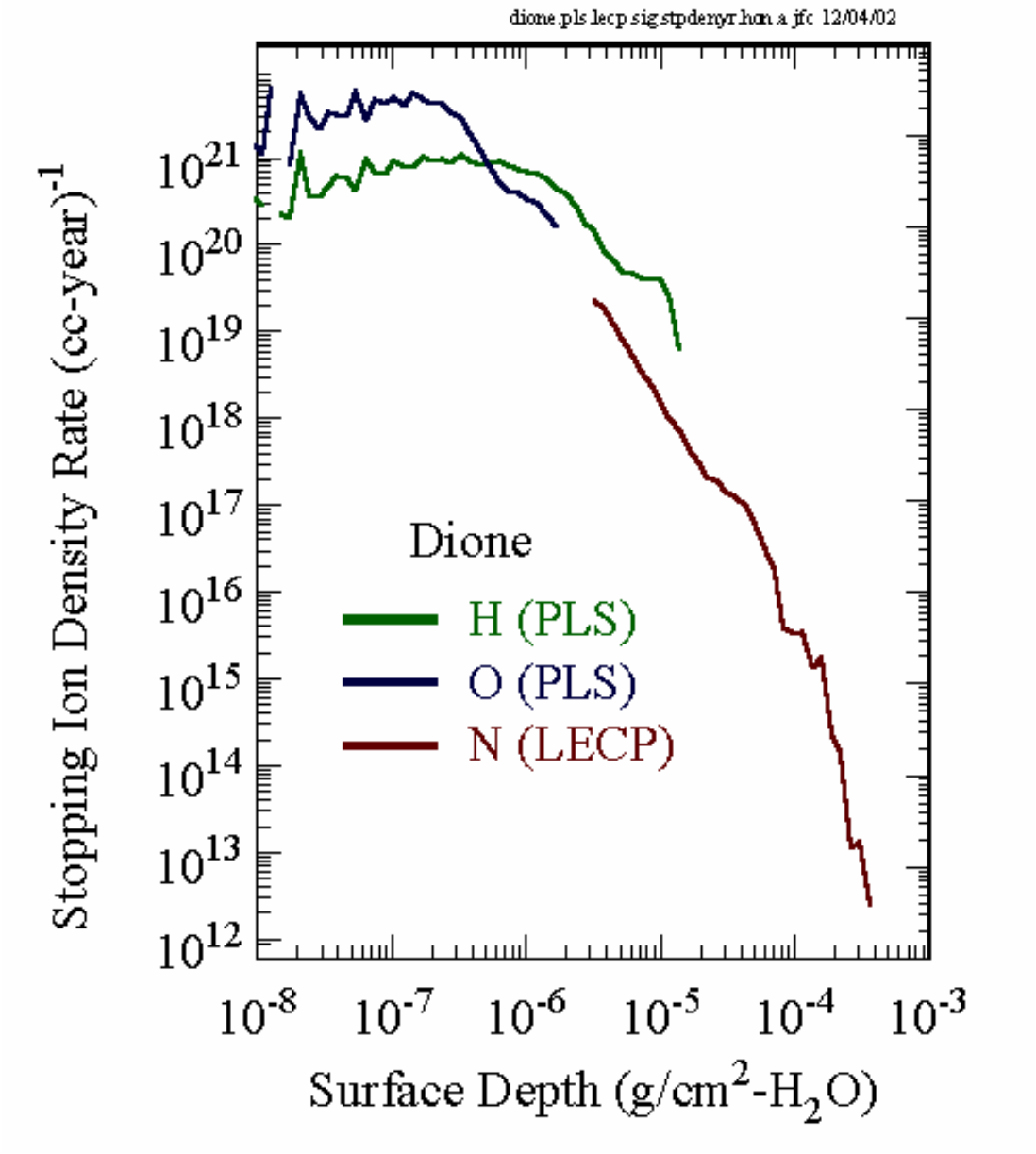
dione.pls lecp sig stpdenyr hon a jfc 12/04/02
Stopping Ion Density Rate (cc-year)-1
10^21
10^20
10^19
10^18
10^17
10^16
10^15
10^14
10^13
10^12
Dione
H (PLS)
O (PLS)
N (LECP)
10^-8
10^-7
10^-6
10^-5
10^-4
10^-3
Surface Depth (g/cm2-H2O)

Figure 11.

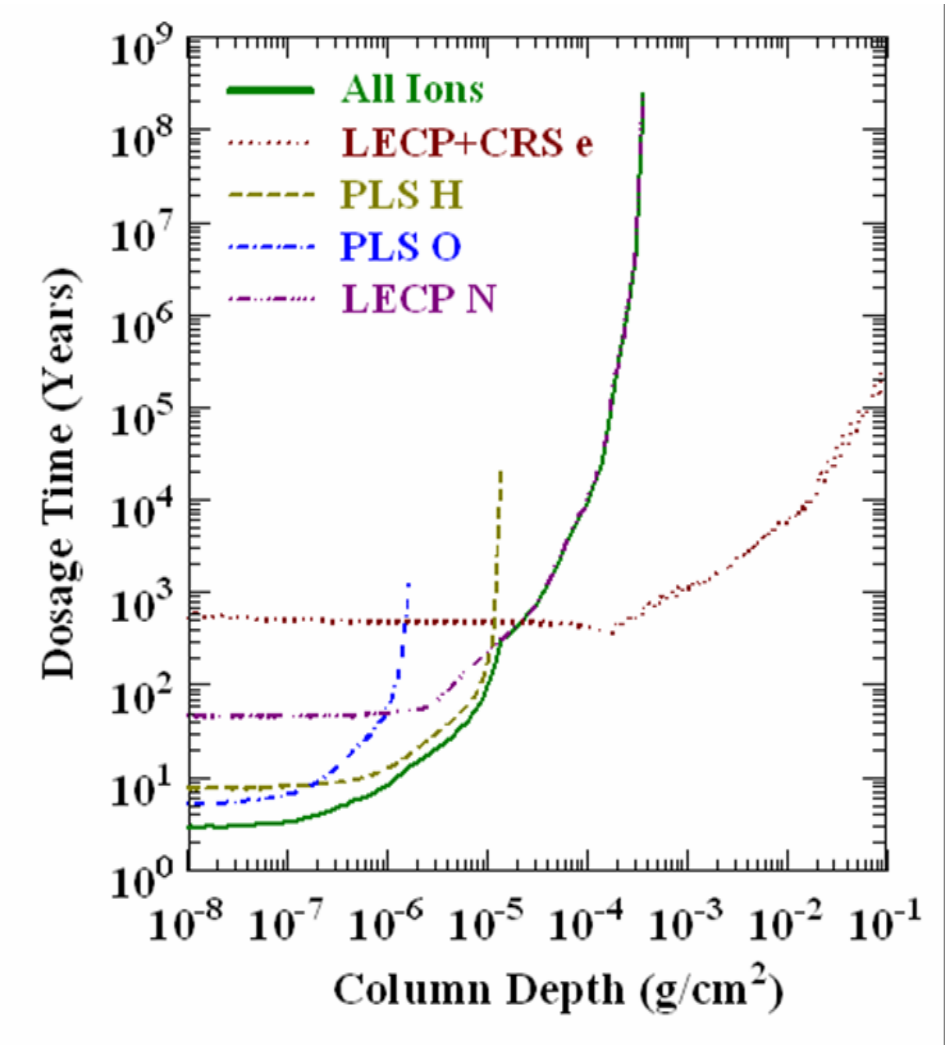
All Ions
LECP+CRS e
PLS H
PLS O
LECP N
Dosage Time (Years)
Column Depth (g/cm²)
10⁹
10⁸
10⁷
10⁶
10⁵
10⁴
10³
10²
10¹
10⁰
10⁻⁸ 10⁻⁷ 10⁻⁶ 10⁻⁵ 10⁻⁴ 10⁻³ 10⁻² 10⁻¹

Figure 12.

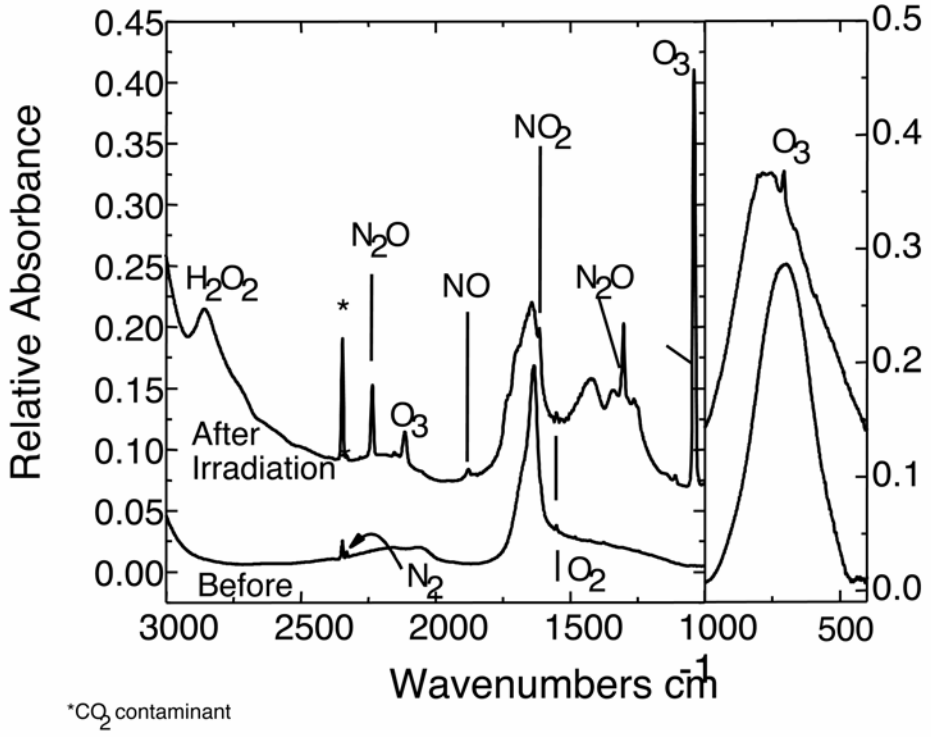
Relative Absorbance
0.45
0.40
0.35
0.30
0.25
0.20
0.15
0.10
0.05
0.00
0.5
0.4
0.3
0.2
0.1
0.0
3000
2500
2000
1500
1000
500
Wavenumbers cm-1
H2O2
*
N2O
O3
NO
NO2
N2O
O3
O3
After
Irradiation
Before
N2
O2
*CO2 contaminant

Figure 13.